



ARL-TR-7630 • MAR 2016



US Army Research Laboratory

A Rugged Ultra-Wideband (UWB) Circular Planar Monopole for Multichannel Radar

by Seth A McCormick, Amir I Zaghloul, and Arthur C Harrison

Approved for public release; distribution unlimited.

NOTICES

Disclaimers

The findings in this report are not to be construed as an official Department of the Army position unless so designated by other authorized documents.

Citation of manufacturer's or trade names does not constitute an official endorsement or approval of the use thereof.

Destroy this report when it is no longer needed. Do not return it to the originator.



A Rugged Ultra-Wideband (UWB) Circular Planar Monopole for Multichannel Radar

by Seth A McCormick, Amir I Zaghloul, and Arthur C Harrison
Sensors and Electron Devices Directorate, ARL

REPORT DOCUMENTATION PAGE				Form Approved OMB No. 0704-0188	
<p>Public reporting burden for this collection of information is estimated to average 1 hour per response, including the time for reviewing instructions, searching existing data sources, gathering and maintaining the data needed, and completing and reviewing the collection information. Send comments regarding this burden estimate or any other aspect of this collection of information, including suggestions for reducing the burden, to Department of Defense, Washington Headquarters Services, Directorate for Information Operations and Reports (0704-0188), 1215 Jefferson Davis Highway, Suite 1204, Arlington, VA 22202-4302. Respondents should be aware that notwithstanding any other provision of law, no person shall be subject to any penalty for failing to comply with a collection of information if it does not display a currently valid OMB control number.</p> <p>PLEASE DO NOT RETURN YOUR FORM TO THE ABOVE ADDRESS.</p>					
1. REPORT DATE (DD-MM-YYYY) March 2016		2. REPORT TYPE Final		3. DATES COVERED (From - To) 07/2015 – 02/2016	
4. TITLE AND SUBTITLE A Rugged Ultra-Wideband (UWB) Circular Planar Monopole for Multichannel Radar				5a. CONTRACT NUMBER	
				5b. GRANT NUMBER	
				5c. PROGRAM ELEMENT NUMBER	
6. AUTHOR(S) Seth A McCormick, Amir I Zaghloul, and Arthur C Harrison				5d. PROJECT NUMBER R.0018185.1.1	
				5e. TASK NUMBER	
				5f. WORK UNIT NUMBER	
7. PERFORMING ORGANIZATION NAME(S) AND ADDRESS(ES) US Army Research Laboratory ATTN: RDRL-SER-M 2800 Powder Mill Rd Adelphi, MD 20783-1138				8. PERFORMING ORGANIZATION REPORT NUMBER ARL-TR-7630	
9. SPONSORING/MONITORING AGENCY NAME(S) AND ADDRESS(ES)				10. SPONSOR/MONITOR'S ACRONYM(S)	
				11. SPONSOR/MONITOR'S REPORT NUMBER(S)	
12. DISTRIBUTION/AVAILABILITY STATEMENT Approved for public release; distribution unlimited.					
13. SUPPLEMENTARY NOTES					
14. ABSTRACT <p>This report presents the design, computational electromagnetic modeling, and measurement of a cavity-backed circular planar monopole antenna intended to serve as an alternative to an already existing Vivaldi antenna in a multichannel radar system. This report briefly summarizes the standard performance and design methods of both a generic circular planar monopole and Vivaldi to give a background on both antennas. The circular planar monopole presented is based on previous work, and is modified through 2 revisions to improve forward radiation, isolation, and ruggedness. The final design is compared to the performance of a simulated Vivaldi example to highlight comparable gain performance in a more compact and lower profile package and is further contrasted with the current Vivaldi. The final design has more forward gain and a more tolerable voltage standing wave ratio with a lower profile than the current Vivaldi antenna.</p>					
15. SUBJECT TERMS ultra-wideband, UWB, circular planar monopole, Vivaldi, multichannel radar, US Army Research Laboratory, ARL					
16. SECURITY CLASSIFICATION OF:			17. LIMITATION OF ABSTRACT UU	18. NUMBER OF PAGES 52	19a. NAME OF RESPONSIBLE PERSON Seth A McCormick
a. REPORT Unclassified	b. ABSTRACT Unclassified	c. THIS PAGE Unclassified			19b. TELEPHONE NUMBER (Include area code) 301-394-2706

Contents

List of Figures	iv
Acknowledgments	vi
1 Introduction	1
2 Fundamental Design and Performance of a UWB-CPM	2
3 Introduction to the Vivaldi Antenna and Contrast to the UWB-CPM	3
4 Baseline UWB-CPM	7
5. First Revision of the UWB-CPM	12
6. Second Revision of the UWB-CPM	21
7. Second Revision UWB-CPM versus the Vivaldi	28
8. Summary and Conclusions	32
9. References	34
Appendix. Detailed Drawings for Each Piece of the Enclosure	37
List of Symbols, Abbreviations, and Acronyms	43
Distribution List	44

List of Figures

Fig. 1	Simulation model of a standard Vivaldi Aerial (left) and a close up of the feed region (right)	4
Fig. 2	Example Vivaldi Aerial simulated return loss and electric current distribution at 600 MHz	5
Fig. 3	Example Vivaldi Aerial simulated gain and FBR with a radiation pattern at 600 MHz. Simulation with the infinite dielectric produces a nonphysical null on boresight.	6
Fig. 4	Baseline dimensions (in inches) with a measurement accuracy within ± 0.005	8
Fig. 5	Simulated and measured return loss for the baseline UWB-CPM with and without a reflector	8
Fig. 6	Baseline simulation model with and without a reflector	9
Fig. 7	Simulated realized gain for the baseline UWB-CPM with and without a reflector at $\theta = 0^\circ$ and $\phi = 90^\circ$	10
Fig. 8	Baseline linear pattern at 300 MHz (left) and reflector electric current distribution at 300 MHz (right)	10
Fig- 9	Simulated realized gain for the baseline UWB-CPM with and without a reflector at $\theta = 30^\circ$ and $\phi = 90^\circ$	11
Fig. 10	Baseline UWB-CPM simulated linear radiation patterns vs. theta at 300, 600, 900, and 1,200 MHz	12
Fig. 11	Baseline UWB-CPM (left) and first revision (right)	13
Fig. 12	Simulated and measured return loss for the baseline and first revision	14
Fig. 13	Baseline (left) and first revision (right) electric (top) and magnetic (bottom) current distributions at 1,200 MHz	14
Fig. 14	Simulated realized gain for the baseline UWB-CPM and first revision without a reflector at $\theta = 0^\circ$ and $\phi = 90^\circ$	15
Fig. 15	Simulated realized gain for the baseline UWB-CPM and first revision without a reflector at $\theta = 30^\circ$ and $\phi = 90^\circ$	16
Fig. 16	Completed enclosure (top left), rigidizer (bottom left), and first revision UWB-CPM inside of enclosure (right)	17
Fig. 17	Simulated and measured first revision UWB-CPM return loss with the enclosure	18
Fig. 18	Simulated realized gain for the first revision UWB-CPM with an enclosure at $\theta = 0^\circ$ and $\phi = 90^\circ$	19
Fig. 19	Simulated realized gain for the first revision UWB-CPM with an enclosure at $\theta = 30^\circ$ and $\phi = 90^\circ$	19

Fig. 20	First revision UWB-CPM and enclosure electric current distribution (left) and linear radiation pattern (right) at 950 MHz	20
Fig. 21	First revision UWB-CPM S21 measurement without an enclosure, with an enclosure, and with a radome.....	21
Fig. 22	Second revision dimensions (in inches) with a measurement accuracy within ± 0.005	22
Fig. 23	Size comparison of the first (right) and second (left) UWB-CPM revisions	23
Fig. 24	Simulated and measured return loss for the first and second revision.....	24
Fig. 25	Simulated realized gain for the first and second revision at $\theta = 30^\circ$ and $\phi = 90^\circ$	24
Fig. 26	Simulated and measured return loss for the first and second revisions with an enclosure	25
Fig. 27	Simulated realized gain for the first and second revision with an enclosure at $\theta = 0^\circ$ and $\phi = 90^\circ$	25
Fig. 28	Simulated realized gain for the first and second revision with an enclosure at $\theta = 30^\circ$ and $\phi = 90^\circ$	26
Fig. 29	First (left) and second revision (right) electric current distribution at 950 MHz	27
Fig. 30	First (left) and second revision (right) linear radiation patterns at 950 MHz	27
Fig. 31	Second revision UWB-CPM S21 measurement without an enclosure, with an enclosure, and with a radome.....	28
Fig. 32	Simulated and measured return loss for the first-generation UWB-CPM and the Vivaldi example.....	29
Fig. 33	Simulated and measured VSWR for the first-generation UWB-CPM and the Vivaldi example	30
Fig. 34	Simulated and measured realized gain for the first-generation UWB-CPM and the Vivaldi example.....	30
Fig. 35	First-generation UWB-CPM and Vivaldi example size comparison....	31
Fig. 36	First-generation UWB-CPM and example Vivaldi antenna in dual-pol configuration size comparison	31
Fig. A-1	Enclosure.....	38
Fig. A-2	Enclosure cover.....	39
Fig. A-3	Enclosure connector isolation plate, part 1	40
Fig. A-4	Enclosure connector isolation plate, part 2	41
Fig. A-5	Enclosure short support cover bracket, left.....	42
Fig. A-6	Enclosure long support cover bracket.....	42

Acknowledgments

We would like to thank William O Coburn for his modeling and design insight and for his additional comments on the report.

1 Introduction

The work documented by this report is based on previous work for ground penetrating radar (GPR) and multi-channel radar applications.^{1,2} The antenna presented is a previously designed ultra-wideband (UWB) circular planar monopole (CPM)² covering the band from 300 to 1,200 MHz. The UWB-CPM is a popular antenna for wideband applications due to its compact size, reduced profile, and broad impedance bandwidth.³ The UWB-CPM addressed in this report is designed to provide an alternative to an already existing Vivaldi antenna platform¹ by offering a lower profile alternative with higher gain. While Vivaldi antennas can be UWB and can have moderate to high gain, they also have a large aspect ratio, particularly in length.³ The UWB-CPM trades length for width and will require a reflector to achieve the desired high gain, but will have a much smaller profile compared to the Vivaldi.

There are some design goals for the UWB-CPM, however, that must be met in order to perform as desired. The first goal is that of a directional pattern with high gain and minimal gain variation over the frequency band of interest (300 to 1,200 MHz). If the antenna is to be used in a pulsed system, minimal gain variation is ideal to properly reconstruct the pulse.² The second goal is to reduce the mutual coupling between antenna elements. The antennas are to be arranged in an array configuration (in the same plane), but used individually in a multichannel fashion with simultaneous sampling. Because of the multichannel configuration, reducing the mutual coupling between elements is desired. Another design goal is to ruggedize the antenna in order to protect it from falls and low velocity debris. A dimensional design goal is to keep the antenna in a package with an area that does not exceed 12 x 12 inches and has a shorter length profile than the current Vivaldi.

The following details the design effort of the first generation of UWB-CPMs to replace an already existing Vivaldi, which includes the required revisions to overcome problems in the design, discussion of design choices, as well as computational electromagnetic modeling (CEM) and measurements. The next section discusses the fundamental performance of a standard UWB-CPM. The third section discusses the standard exponentially tapered Vivaldi antenna and contrasts the size and performance to the UWB-CPM using a simulated example Vivaldi. The example Vivaldi is not the same as the existing antenna, as the current antenna is much smaller than the example. Sections 4–7 discuss the baseline, first, and second revisions made to meet the design requirements, including a discussion of the CEM modeling process used to achieve the best possible agreement with measurement for each revision.

Section 9 compares the second revision UWB-CPM to the example Vivaldi and contrasts that comparison to the current Vivaldi. The last section concludes and summarizes the design effort and performance of the delivered antennas. Note that all simulations were done using the Method of Moments (MoM) full-wave solver in the CEM code FEKO.⁴

2 Fundamental Design and Performance of a UWB-CPM

The classic quarter-wave monopole antenna is a quarter-wavelength-long wire fed (typically at the base) against a large ground plane. The monopole antenna exhibits a narrow bandwidth and a half-sphere radiation pattern with a typical realized gain of about 5.1 dBi.⁵ By enlarging the diameter of the quarter-wave monopole or using a different geometry (i.e., a sphere), the impedance bandwidth can be increased.^{5,6} The size of the quarter-wave monopole can be reduced by projecting the 3-dimensional (3-D) structure onto a 2-dimensional plane, creating a planar monopole, with a corresponding change in the feeding mechanism.

If the 3-D quarter-wave monopole is wide or spherical, the planar monopole will have an impedance bandwidth similar to the 3-D structure. The planar monopole can be of many different shapes, but typically the one with the largest impedance bandwidth and best pattern stability is the circular monopole.^{7,8} The diameter of the monopole is set such that the circumference is approximately a wavelength (with a correction for the wavelength due to the dielectric),

$$C = \pi d = \lambda_{eff} \rightarrow d = \frac{\lambda_{eff}}{\pi}, \quad (1)$$

where C is the circumference, d is the diameter, and λ_{eff} is the effective wavelength adjusted for the dielectric. The diameter is bounded by upper and lower values defined by the free-space wavelength and dielectric wavelength, respectively. The dielectric correction is captured by the effective permittivity, which is commonly approximated by an infinite half-space (i.e., $\epsilon_{eff} = \frac{1+\epsilon_r}{2}$). Note that it is not unusual for the infinite half-space approximation to yield an overestimate.

A planar UWB monopole can be fed by using a co-planar waveguide (CPW), a microstrip, or a pin feed using a coaxial cable center conductor. For the CPW, the antenna is fed against a ground plane that is in the same plane as the antenna. The ground plane and antenna are separated by a small gap with a dimension that is significantly smaller than the low frequency wavelength (approximately 700 times smaller for the antenna in this report). The width and length of the ground can have a significant effect on the performance of the monopole.^{9,10} Typically, the width across the substrate should be no larger than approximately 20% larger than the

monopole diameter (roughly a quarter-wave at the lowest frequency), and the length should be no smaller than a quarter of the monopole diameter. If the ground width is too large or the length too small, the monopole can have serious pattern instabilities and/or will not be matched to $50\ \Omega$.^{9,10} The CPM can easily cover a 4:1 impedance bandwidth and can be improved further through modifications to the ground plane, such as rounding the ground plane away from the monopole and strategic notching.^{9,10}

The radiation pattern, however, is not stable with frequency and can change significantly over the impedance bandwidth of interest. At low frequencies, the radiation pattern is dipole like, but tilts off boresight away from the feed (which is caused by the feed itself) with increase in frequency, usually beginning at the start of the second octave. As frequency increases to the last half of the second octave, the radiation pattern begins to bifurcate. Over a 10:1 impedance bandwidth, the planar monopole has a great deal of gain variation on boresight due to the pattern instability, making the antenna unsuitable for directional applications over a decade bandwidth. Over a 4:1 frequency bandwidth, such as that considered in this report, however, the monopole may be suitable for directional applications, if care is taken in the design.

3 Introduction to the Vivaldi Antenna and Contrast to the UWB-CPM

In 1979, PJ Gibson introduced the Vivaldi Aerial antenna as a new moderate to high gain (10 dBi or greater) wideband antenna (5:1 or greater) with low side lobes (-20 dB side lobe level) and linear polarization that radiates quasi-transverse electromagnetic (TEM) waves.¹¹ The Vivaldi Aerial is also referred to as an end-fire tapered slot antenna with an exponential taper. The antenna functions on the principle of a traveling wave where the electromagnetic waves launched by the feed are guided toward the end of the structure without any reflections (if reflections did occur, then a standing wave would be created). By comparison, a resonant antenna creates standing waves due to reflections at the tips of the antenna. The lack of standing waves is one reason that the Vivaldi Aerial has broadband performance.

The Vivaldi Aerial falls into the “surface wave” category of traveling wave antennas (or slow waves), where the phase velocity is less than the speed of light ($v_{ph} < c$). The other class is known as “leaky wave” antennas (or fast waves), and they require a phase velocity greater than the speed of light ($v_{ph} > c$). Surface wave antennas produce end-fire radiation, which is, of course, the behavior of the Vivaldi radiation pattern.¹² A traveling wave antenna can be created by attenuating the reflections caused by the ends (or tips) of an antenna. This can be accomplished by

either making the antenna very long (greater than one half wavelength) or attaching matched loads to the ends of the antenna.⁵ For the long antenna case, such as the Vivaldi, the length should be sufficiently long (typically greater than 2λ) to minimize the always existent minute reflections that can hamper performance. A classic example of the matched load case is the log periodic dipole array, which uses matched dipoles (logarithmic in size and spacing) to direct a traveling wave.

The original concept of the Vivaldi Aerial from Gibson made use of an exponential taper:

$$y = \pm Ae^{px}, \quad (2)$$

where y is the half separation distance between the tapered edges, x is the length, and p is the exponential growth parameter that governs how quickly or how slowly the tapered slot expands.¹¹ If the exponential growth is too large or too small, then the voltage standing wave ratio (VSWR) can be negatively influenced. Yngvesson et al.¹² parametrically determined that the opening rate of the taper should be at least 0 and less than 0.8 to guarantee proper VSWR (<2.0). Other tapers, such as a linear taper (opening rate of 0) or stepped, can also be found in the literature, but the current antenna uses an exponential taper.^{1,12}

The Vivaldi radiates in the end-fire direction away from the feed. This makes the Vivaldi ideal for applications where directionality and a high front-to-back ratio are required. Figure 1 shows the FEKO simulated model of an exponentially tapered Vivaldi Aerial designed for 300–1,200 MHz and the feed region. Again, this is not the same Vivaldi as the current antenna. The feed region is critical to the performance of the antenna, and it is the transition to flared microstrip that helps to give the Vivaldi a broad impedance bandwidth.¹³ The purpose of this example Vivaldi is to highlight the size and performance if designed according to previous efforts.^{11–13} The current Vivaldi platform¹ is smaller than the example Vivaldi and thus performs better at higher frequencies than at lower frequencies due to the smaller width and length.

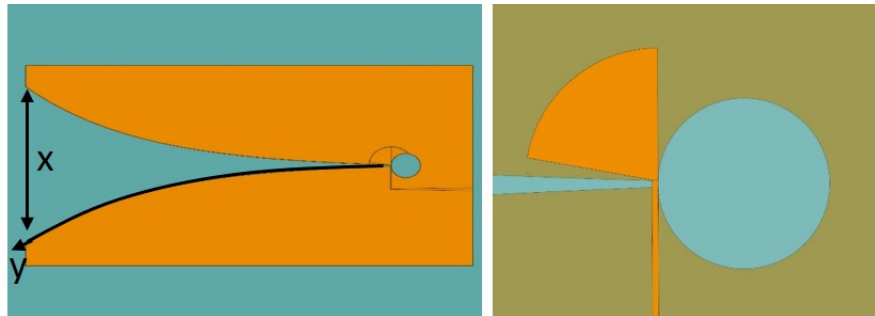


Fig. 1 Simulation model of a standard Vivaldi Aerial (left) and a close up of the feed region (right)

The width of the slot aperture opening sets the low frequency cutoff by being at least a half-wavelength in dimension. The dimensions of the example Vivaldi are approximately 43.43 x 23.45 x 0.120 inches (length x width x depth). The opening width is approximately 18.55 inches and the tapered length (measured from slot opening to end) is 35.1 inches, being roughly a half-wavelength in width and a full-wavelength in length. This example Vivaldi was created using Antenna Magus¹⁴ and was simulated using an infinite dielectric substrate to reduce computation time. Because of the infinite dielectric, material losses could not be included.

Figure 2 shows the return loss of the example Vivaldi Aerial. It is clear that the Vivaldi has a very good impedance match to 50 Ω (return loss ≤ -10 dB) across the 4:1 frequency band with a small peak at about 400 MHz. The realized gain is relatively high for most of the frequency band (Fig. 3). The peak gain rises from 4.5 dBi to about 11.5 dBi across the frequency band and remains flat at 11.5 dBi between 900 and 1,200 MHz. The gain oscillation on boresight is due to pattern wobble, where the beam peak location changes with frequency. Also shown is the front-to-back ratio (FBR), where the value oscillates around 15 dB. The reason why the FBR is lower than what would be typical of a Vivaldi is due to the fact that the length of the taper is only a full-wavelength at cutoff instead of being at least 2 wavelengths.

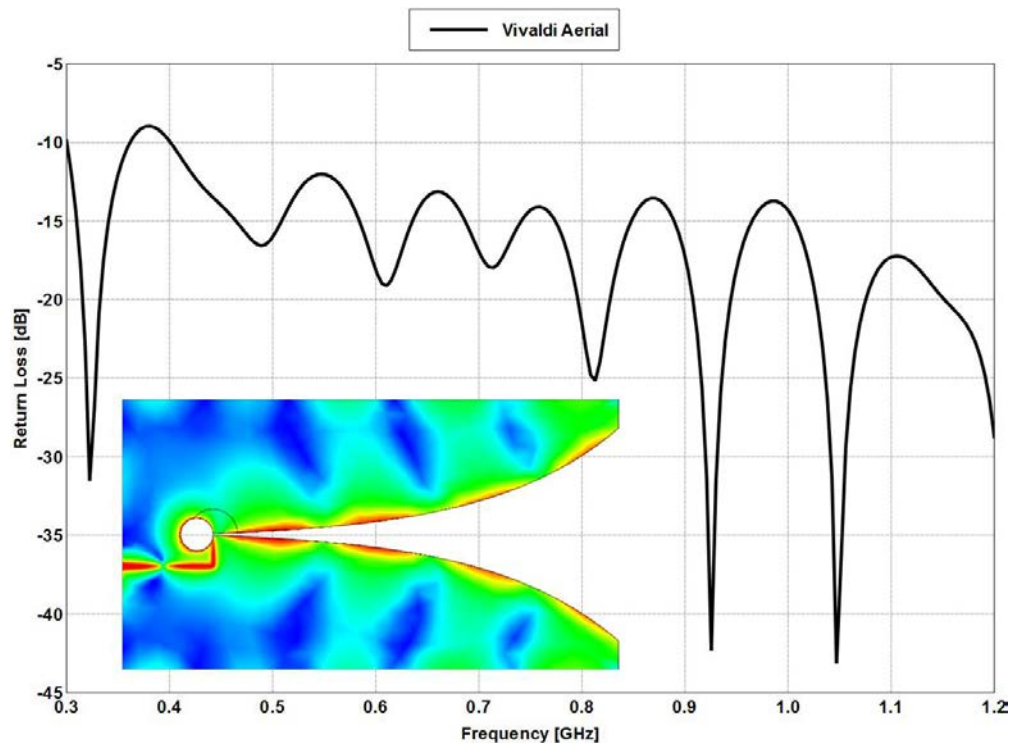


Fig. 2 Example Vivaldi Aerial simulated return loss and electric current distribution at 600 MHz

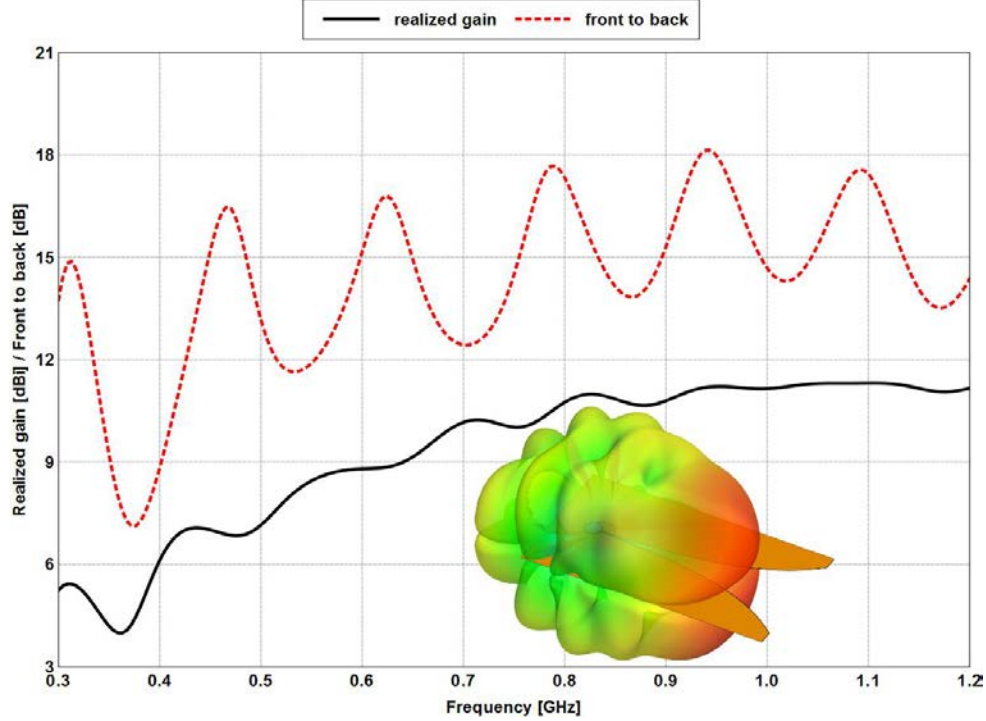


Fig. 3 Example Vivaldi Aerial simulated gain and FBR with a radiation pattern at 600 MHz. Simulation with the infinite dielectric produces a nonphysical null on boresight.

Increasing the length of the Vivaldi would subsequently increase the forward directivity and thus the gain and FBR. It is well understood that for traveling wave antennas with a constant phase velocity, the directivity is proportional to the length-to-wavelength ratio (i.e., $A \frac{L}{\lambda}$). The constant of proportionality is approximately 10 for traveling wave antennas with lengths between 3λ and 8λ and scales as \sqrt{L} .¹¹ The Vivaldi Aerial does not have a constant phase velocity, however, due to the exponential taper, but the variation is small. The non-constant phase velocity causes the directivity to deviate from the approximation, but the approximation is still valid. Although the directivity may be predictable from the dimensions, the electric (E)- and magnetic (H)-plane beam widths may not be. The length, permittivity, and dielectric thickness of the antenna play critical roles in governing the E- and H-plane beam width behavior. From Yngvesson et al.,¹² it is understood that as a rule of thumb, a shorter Vivaldi can tolerate a thicker dielectric and a longer Vivaldi will require a thinner dielectric to maintain E and H beam width stability.

While the Vivaldi shows very good broadband performance with high gain even with a 1λ length, there is an obvious drawback in terms of size. At 43.43 x 23.45 inches, the 300-MHz Vivaldi has a large length and width. For a comparable UWB-CPM, the diameter would be between 8.21 and 12.53 inches (considering the same dielectric) with a ground plane width between 9.85 and 15.04 inches and length

between 2.05 and 3.13 inches (using the design rules of thumb mentioned in Section 2). Comparing the dimensions of the UWB-CPM (between 9.85 x 10.26 inches and 15.04 x 15.67 inches) to the dimensions of the Vivaldi Aerial (43.43 x 23.45 inches), it is clear that the UWB-CPM is more compact for the same low frequency and dielectric. The CPM orientation will produce a profile with greater breadth than the Vivaldi; however, the peak gain is almost always broadside instead of end-fire. Thus, while the depth will be smaller for the UWB-CPM, the surface area may not be. If a dual-polarized (dual-pol) configuration was used, however, then the UWB-CPM would be smaller in all dimensions, as is shown at the end of this report.

A downside to the small size is that the UWB-CPM has less gain. Without a reflector (or cavity backing), the UWB-CPM would only have a peak realized gain of about 3 dBi and does not have an as well-behaved radiation pattern as the Vivaldi. The loss in the gain can be accepted, however, given that even with a reflector (or cavity) the vertical profile of the UWB-CPM could be at least a factor of 3 times smaller than the Vivaldi. As is shown later, the designed UWB-CPM has comparable gain to the example Vivaldi with a smaller package and, by extension, clearly outperforms the current Vivaldi that is smaller than the example.

4 Baseline UWB-CPM

The baseline UWB-CPM is a basic CPM without any modifications made to the ground plane and fed using a CPW feed with an edge connector. It is a 300-MHz version of a previous UWB-CPM² for handheld use. Fig. 4 shows the full list of its dimensions. The dielectric substrate is Rogers RO 4350b ($\epsilon_r = 3.48$ and $\tan\delta = 0.0037$) with 0.5-oz copper cladding and no finish. Zaghloul et al.² made use of a multi-layered electromagnetic bandgap (EBG) backing and director element to improve the magnitude of the forward gain and minimize the variation, which was successful, but the additional layers increased the vertical profile. Even without the director, the multi-layered EBG could still produce a large profile comparable to a quarter-wave reflector. A single layer EBG can reduce the profile of a narrowband antenna beyond that of a quarter-wave reflector, but to achieve a broadband EBG, multiple layers are required, which will undoubtedly increase the vertical profile.

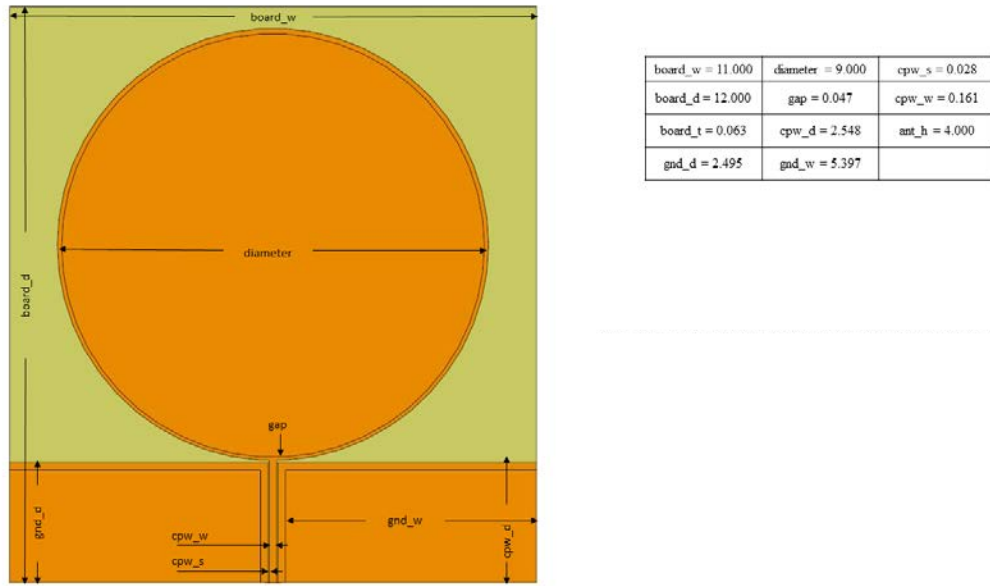


Fig. 4 Baseline dimensions (in inches) with a measurement accuracy within ± 0.005

To keep the vertical profile small, a 12 inch x 12 inch quarter-wave reflector and plastic enclosure were decided upon to improve the gain in the forward direction and provide protection for the antenna element. Figure 5 shows the return loss for the baseline configuration with and without the 12 inch x 12 inch quarter-wave reflector behind the antenna. Figure 6 shows the simulation model constructed and meshed with FEKO.

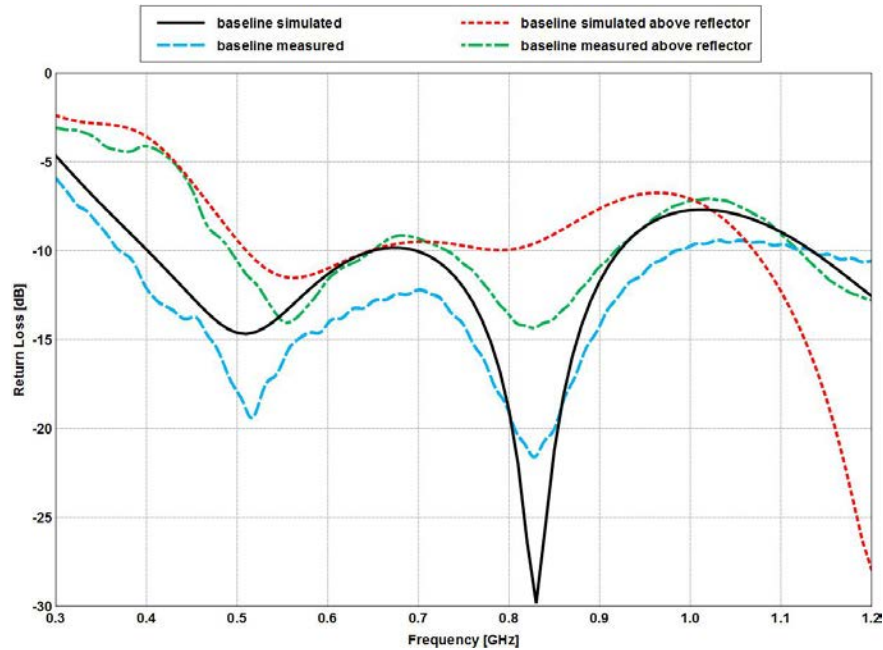


Fig. 5 Simulated and measured return loss for the baseline UWB-CPM with and without a reflector

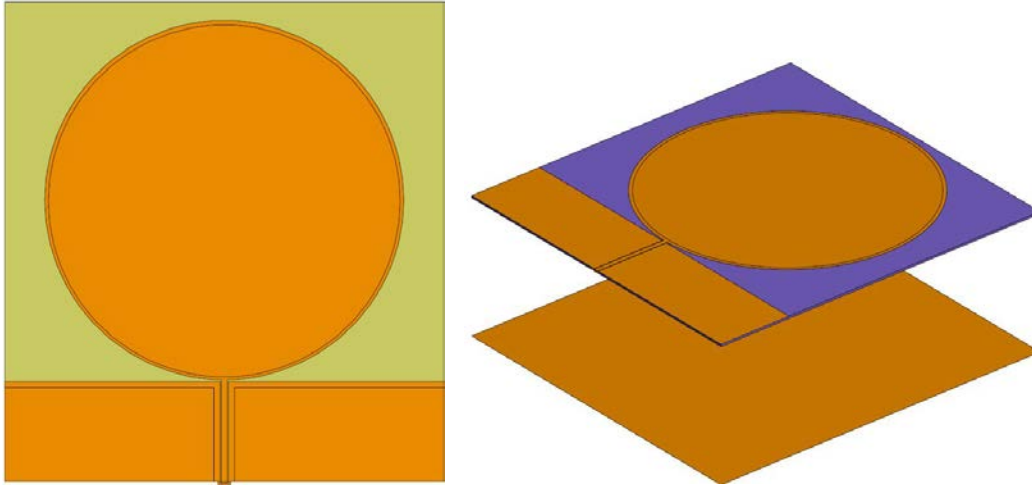


Fig. 6 Baseline simulation model with and without a reflector

The baseline UWB-CPM shows a good broadband 50- Ω match across the frequency range of 350 to 1,200 MHz. The inclusion of the quarter-wave reflector harms the match below 500 MHz. This is to be expected, as the spacing between the reflector and antenna was chosen to be quarter-wave at 750 MHz, which would naturally lend to a poor return loss at frequencies where the spacing approaches $\frac{\lambda}{8}$ and smaller. The realized gain for the baseline UWB-CPM, shown in Fig. 7, is about 3 dBi without the reflector between 400 and 700 MHz. The roll-off in gain below 400 MHz is due to the poor return loss, but the roll-off in gain above 700 MHz is due to E-plane beam tilt from broadside. The inclusion of the quarter-wave reflector improves the gain between 400 and 700 MHz by about 4 dBi, but still roll-offs below 400 MHz (which is more severe) and above 700 MHz. The gain also varies by about 16 dBi with and without the reflector.

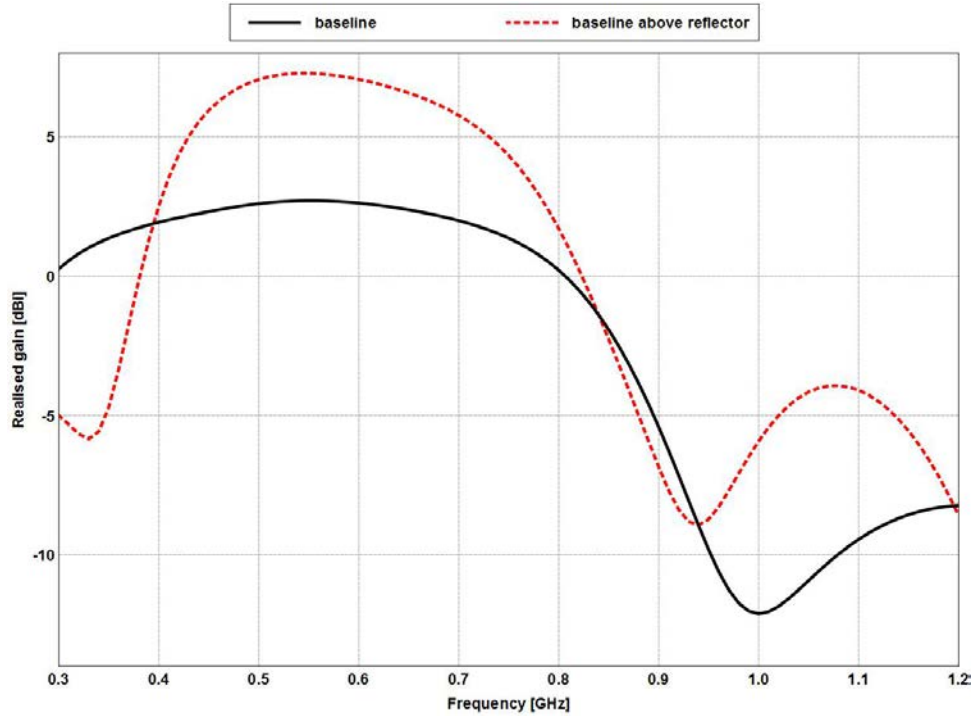


Fig. 7 Simulated realized gain for the baseline UWB-CPM with and without a reflector at $\theta = 0^\circ$ and $\varphi = 90^\circ$

The gain roll-off when the quarter-wave reflector is included is due in part to the poor return loss, but is mostly caused by the fact that the reflector is the dominate radiator at low frequencies. Figure 8 shows the linear pattern and the electric current distribution on the reflector at 300 MHz. From both the linear pattern and the current distribution, it is clear that the main culprit for the roll-off in realized gain at low frequencies is the radiating reflector. Below 400 MHz, the 12 inch x 12 inch reflector is much too small to perform properly and would need to be quite a bit larger in order to fix the backward-facing radiation pattern.

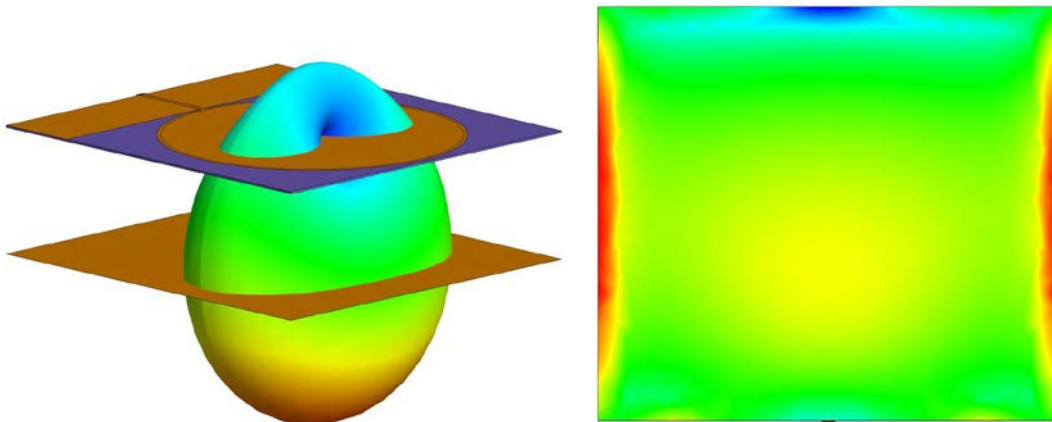


Fig. 8 Baseline linear pattern at 300 MHz (left) and reflector electric current distribution at 300 MHz (right)

The low realized gain above 700 MHz can be rectified by tilting the antenna and reflector (in theta) to the angle at which the peak realized gain over the frequency band can be realized. The E-plane tilt angle was determined to be approximately 30° (in theta) away from the feed. Figure 9 shows the realized gain at $\theta = 30^\circ$ for the baseline antenna with and without the reflector. At this tilt angle, the gain across the frequency band does not vary as much. Without the reflector, the gain varies by about 5 dBi, and with the reflector, the gain varies by about 2 dBi above 500 MHz. Below 500 MHz, the gain with the reflector has the same problem mentioned previously. Figure 10 shows the linear E-plane radiation patterns at 300, 600, 900, and 1,200 MHz to highlight the beam tilt, away from the feed, with frequency.

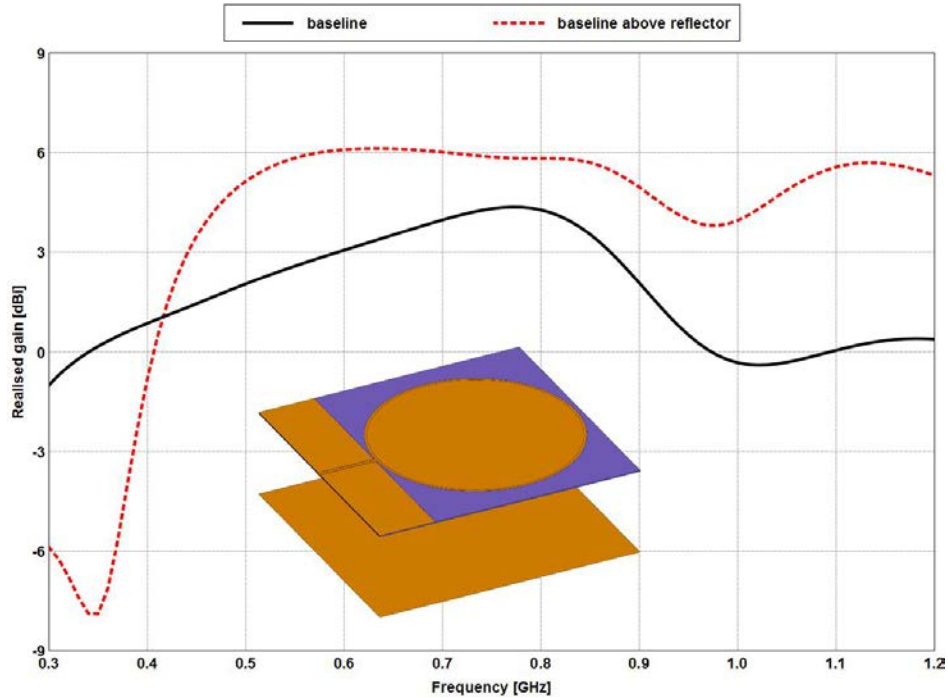


Fig- 9 Simulated realized gain for the baseline UWB-CPM with and without a reflector at $\theta = 30^\circ$ and $\phi = 90^\circ$

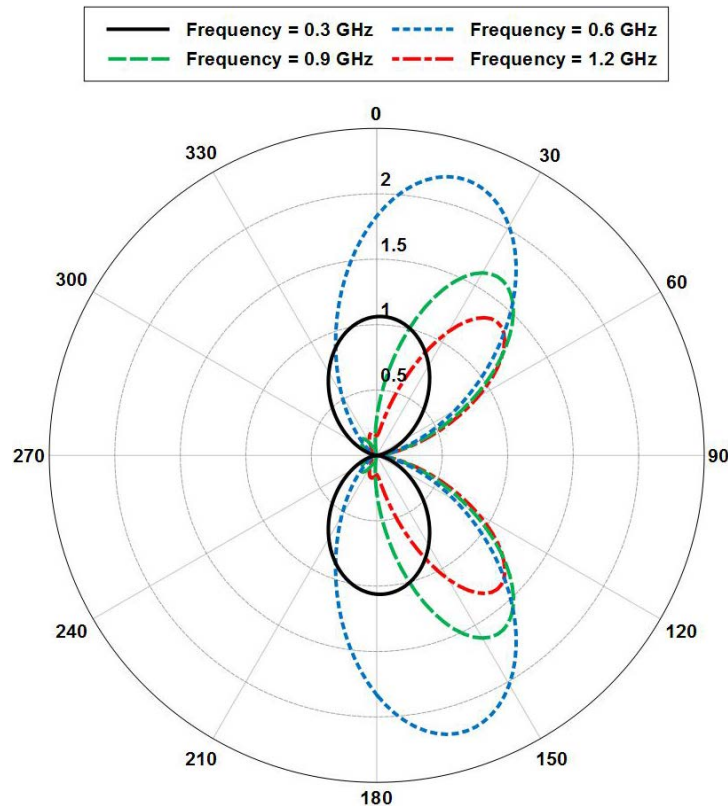


Fig. 10 Baseline UWB-CPM simulated linear radiation patterns vs. theta at 300, 600, 900, and 1,200 MHz

While the baseline CPM shows good performance across the bandwidth of interest, there are a few issues that need to be addressed. The first, and most obvious issue, is that the backward-facing radiation pattern due to the small reflector hinders performance. At the very least, the reflector needs to be enlarged to address this problem. The other issue is that of the plastic enclosure. Two of the design goals necessitated a rugged antenna with low mutual coupling between elements. While structural grade plastics, such as G10, are sturdy, they are also very heavy and would require thick walls. Also, the plastic would not help to reduce the mutual coupling between antenna elements. The solution presented here is to use a metallic enclosure for each element.

5. First Revision of the UWB-CPM

As mentioned in Section 2, the return loss of a UWB-CPM can be improved with modification to the planar ground plane. The ground plane in the first revision is rounded away from the feed to help improve the return loss. Also, 0.5 inch of excess substrate was removed from the top to reduce the overall length. Figure 11 shows a side-by-side comparison of the baseline and first revision. All of the dimensions

are the same as the baseline with the exception of the following: $\text{board_d} = 11.500$, $\text{cpw_w} = 0.155$, $\text{cpw_s} = 0.011$, and $\text{ant_h} = 4.829$. The CPW was adjusted to better match to a $50\text{-}\Omega$ impedance, and the increase in antenna spacing was, in part, a compromise to trade off a small increase in vertical profile and a small decrease in gain for a potential improvement in return loss. The dielectric remains the same, as does the copper thickness, but the first revision has a silver finish instead of none.

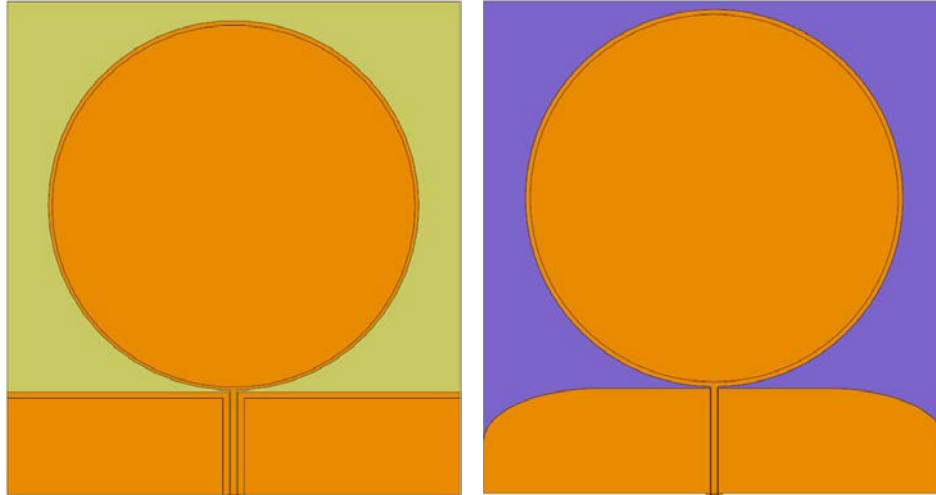


Fig. 11 Baseline UWB-CPM (left) and first revision (right)

The rounding was achieved using an ellipse with a major radius of 2.75 inches and a minor radius of 1.25 inches centrally located on each half of the ground plane. The curvature and CPW adjustment improves the return loss across the band, as seen in Fig. 12, with the best improvement at frequencies above 900 MHz. As a point of fact, the feed model for the black and red curves are the same, but as can be seen from Fig. 12, it was necessary to change the feed model for the first revision to an approximate coaxial end launch to obtain better agreement with the measurement, although the simulated impedance can no longer be attained due to the waveguide port. The electric and magnetic current distributions for the baseline and first revisions (Fig. 13) show that the curvature of the ground plane increases the apparent length. The longer current path allows for a smoother transition from the feed region to the outer portion of the ground plane.

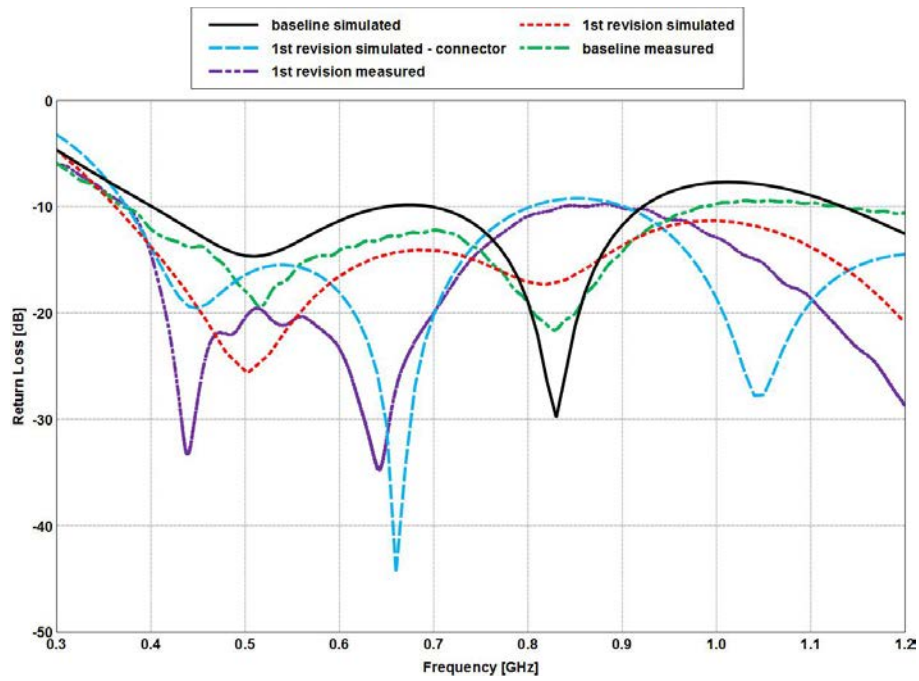


Fig. 12 Simulated and measured return loss for the baseline and first revision

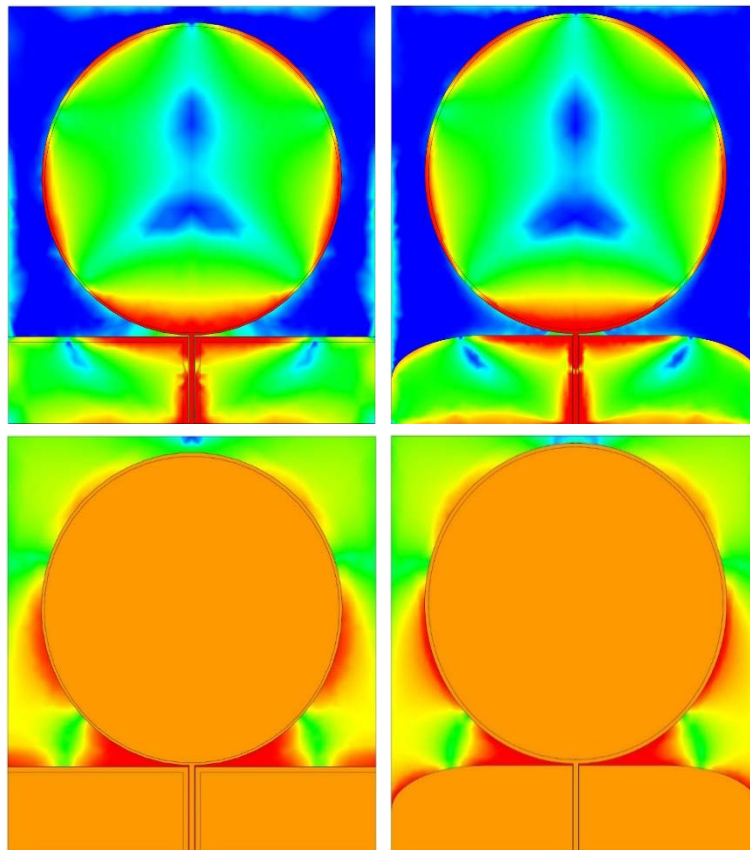


Fig. 13 Baseline (left) and first revision (right) electric (top) and magnetic (bottom) current distributions at 1,200 MHz

Like the return loss, the gain did not improve at low frequencies with the rounding of the ground plane (Figs. 14 and 15). The best improvement can be seen at frequencies above 900 MHz, where the improvement is about 1 dBi. Below 900 MHz, the gain improvements amounts to fractions of a decibel isotropic. Although the rounding did not drastically improve the performance of the UWB-CPM, it does help to maximize the performance without optimization.

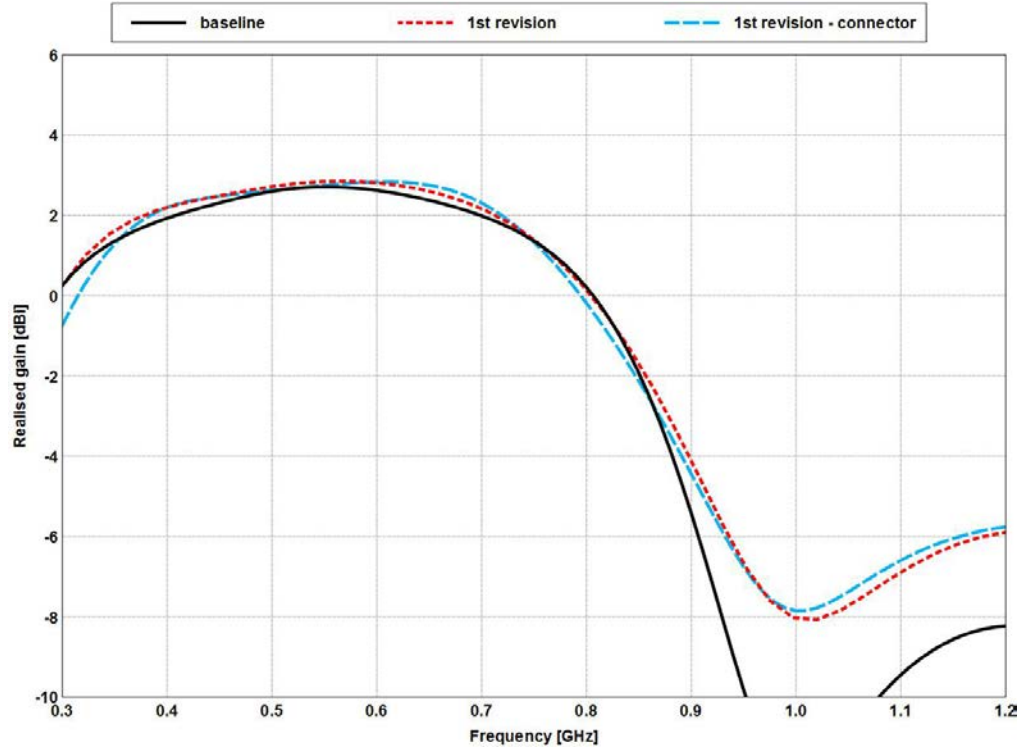


Fig. 14 Simulated realized gain for the baseline UWB-CPM and first revision without a reflector at $\theta = 0^\circ$ and $\varphi = 90^\circ$

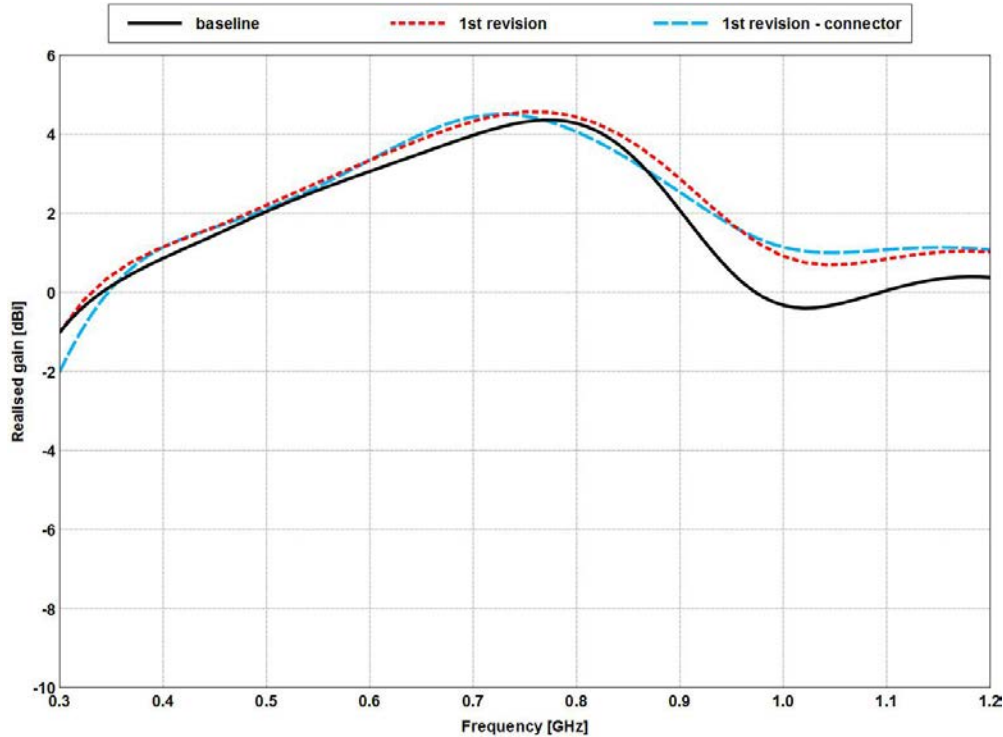


Fig. 15 Simulated realized gain for the baseline UWB-CPM and first revision without a reflector at $\theta = 30^\circ$ and $\phi = 90^\circ$

Because of the problems with the plastic enclosure mentioned at the end of Section 4, an alternative metallic enclosure assembled in house had to be used. The custom ordered metallic enclosure is made of welded aluminum measuring 12 inches x 12 inches x 5 inches x $\frac{3}{32}$ inch (with respect to the inside). The enclosure is capped by white structural-grade polycarbonate to protect the antenna from debris and falls. The polycarbonate is attached to the metallic enclosure using aluminum right angles that are bolted to the enclosure walls. The antenna is inset from the top of the enclosure by about 0.1715 inches in order to hide the end launch connector beneath the polycarbonate and is displaced from the wall at the feed location by about 0.125 inches. The antenna is centered along the axis parallel to the feed location and sits atop a stack of polystyrene foam with another thin layer of foam on top of the antenna to protect and apply compression when the polycarbonate is attached. See the Appendix for detailed drawings for each piece of the enclosure.

During the beginning of the prototyping phase, the outer conductor of the end launch connector was soldered directly to the nearby enclosure wall for structural support. This was not ideal, however, as the connection to the nearby wall drove the antenna against the enclosure instead of just the CPW ground plane, severely harming the return loss. To maintain a rigid support for the connector while keeping

the wall isolated from the connector, a cutout measuring 2 inches x 1.5 inches was made, around the feed region, in the nearby enclosure wall. A plate of G10 was then bolted to the wall with a U-shaped brass piece bolted to the G10 plate. The outer conductor of the connector was then soldered to the brass piece. Figure 16 shows the completed enclosure, the rigidizer for the feed, and the first revision UWB-CPM inside of the enclosure.



Fig. 16 Completed enclosure (top left), rigidizer (bottom left), and first revision UWB-CPM inside of enclosure (right)

The measured and simulated return loss for the first revision UWB-CPM inside of the enclosure (Fig. 17) shows a good match at 550 MHz and above. This is a bandwidth retention of 81.25% of the first revision impedance bandwidth without the enclosure. Modeling shows relatively good agreement with measurement, but the expected return loss was worse than measured. Including the enclosure thickness had some impact on the agreement with measured data, but overall, did not improve the agreement enough to justify the increase in memory and computation time. Including the rigidizer and mesh refinement did not account for the discrepancy between the simulation and measurement.

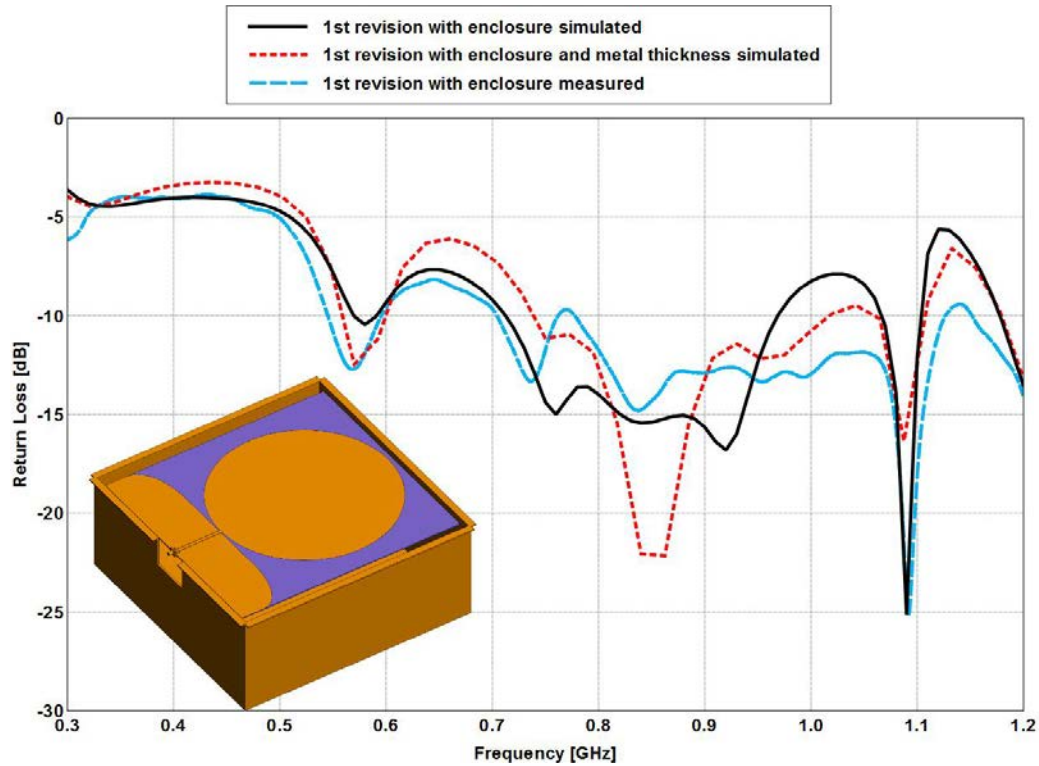


Fig. 17 Simulated and measured first revision UWB-CPM return loss with the enclosure

Figures 18 and 19 show the realized gain versus frequency at $\theta = 0^\circ$ and $\theta = 30^\circ$. Clearly, the metallic enclosure solves the problem of low gain below 400 MHz, but now the gain has 3 large dips at 600, 950, and 1,050 MHz. The dip at 600 MHz is due to the pattern tilt, which has been discussed previously, but the dips at 950 and 1,050 MHz are not due to beam tilt nor are they due to a poor return loss. The dips at 950 and 1,050 MHz come from the interaction between the UWB-CPM and the enclosure, which produces a bifurcated radiation pattern at those frequencies. The electric current distribution and linear radiation pattern at 950 MHz (Fig. 20) show that the edges of the enclosure have a similar current distribution as the antenna. The edges of the enclosure radiate in a way that reinforces the beam splitting of the antenna, thereby creating a dip in the gain.

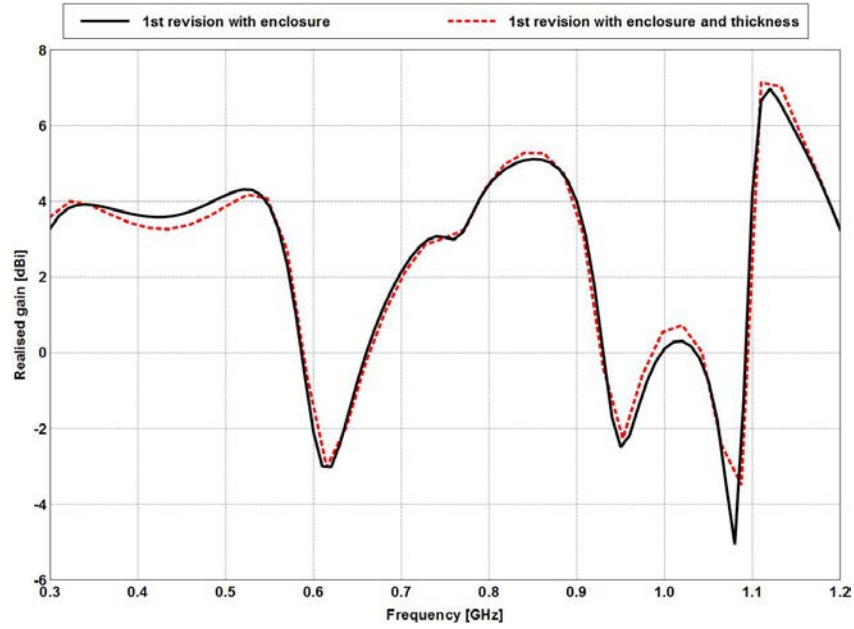


Fig. 18 Simulated realized gain for the first revision UWB-CPM with an enclosure at $\theta = 0^\circ$ and $\phi = 90^\circ$

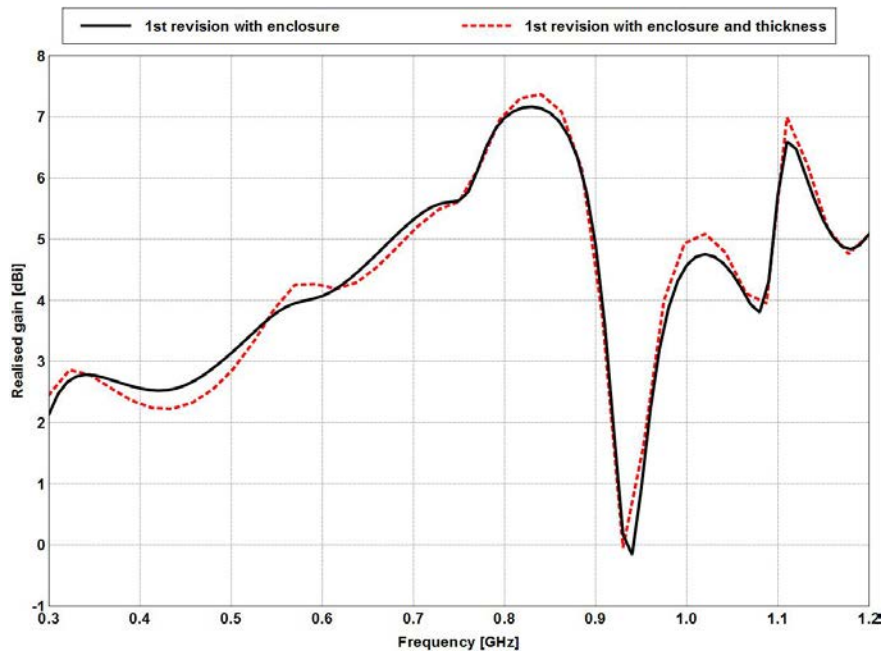


Fig. 19 Simulated realized gain for the first revision UWB-CPM with an enclosure at $\theta = 30^\circ$ and $\phi = 90^\circ$

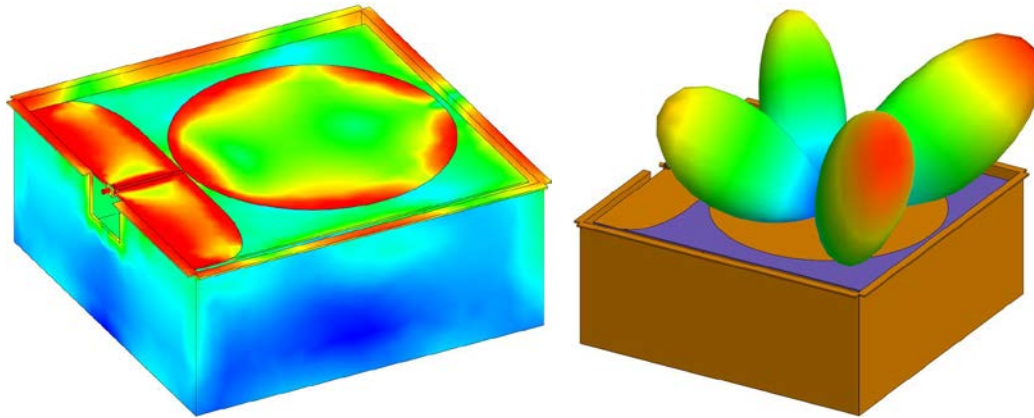


Fig. 20 First revision UWB-CPM and enclosure electric current distribution (left) and linear radiation pattern (right) at 950 MHz

To mitigate the beam splitting, time was spent trying to modify the enclosure in such a way as to lengthen, shorten, or attenuate the current path along the edges of the enclosure. Simulations with a commercial-grade absorber on the enclosure edges did not attenuate the current and so did not help with the beam splitting. Applying notches to the enclosure walls did have an effect. Depending on where the notches were placed, the impedance or the radiation pattern could be affected.

From the electric current distribution in Fig. 20, the edge that carries the most current is the one adjacent to the feed. The first round of notching consisted of applying 2 notches located on either side of the feed and adjusting the position, but while there was an appreciable effect on the radiation pattern, to be successful required wide notches placed away from the feed. This configuration resulted in a return loss that was too poor to be of any use. Applying notches to any of the other 3 sides had similar results.

Because modifications to the enclosure did not fix the dips in gain, the only other option was to modify the antenna. If the antenna was reduced in size so that the bifurcation occurred at frequencies higher than the maximum frequency in band, then the gain with the enclosure would not have the dips. The metallic enclosure did improve the isolation between the antennas, however, as can be seen in the S21 measurement (Fig. 21).

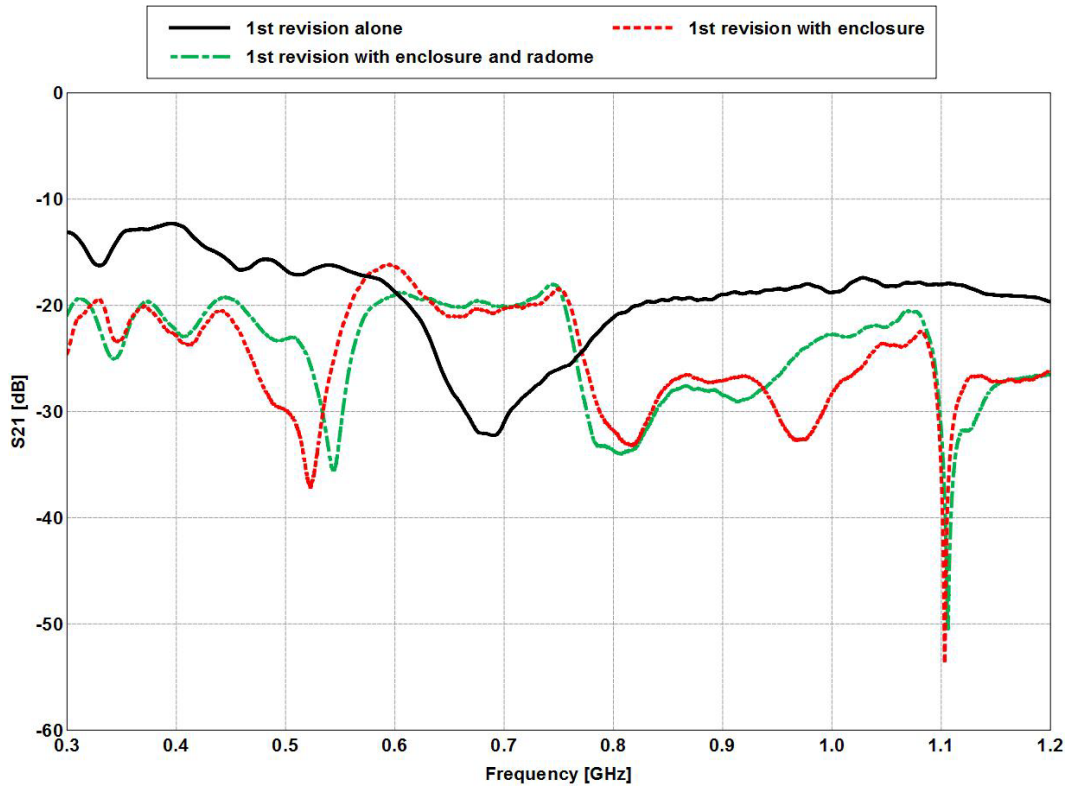


Fig. 21 First revision UWB-CPM S21 measurement without an enclosure, with an enclosure, and with a radome

The S21 measurement was made under anechoic conditions with 2 antennas separated by a distance of 13.5 inches center-to-center or 0.75 inches edge-to-edge. Without the enclosures, the S21 is, at worst, -12 to -13 dB below 600 MHz and about -18 to -19 dB above 800 MHz. In between 600 and 800 MHz, there is a dip in the S21 where the value minimizes to about -32 dB at 700 MHz. With the enclosure, the S21 is about -20 dB or better across the entire frequency band even though the S21 at 700 MHz is now -20 dB instead of -32 dB. The loss in isolation at 700 MHz is most likely a resonant effect of the enclosures and the interaction between them. Including the radome has some effect on the S21, but still maintains a value of about -20 dB or better. Even though the enclosure improves the isolation, the dips in gain are not acceptable. The second revision of the UWB-CPM addresses this problem.

6. Second Revision of the UWB-CPM

As shown in Section 5, the first revision of the UWB-CPM has gain dips at 950 and 1,050 MHz due to interactions with the enclosure that result in a bifurcated radiation pattern. All attempts to mitigate the dips through modification of the enclosure failed, so the only thing left to modify was the antenna itself. The simplest

modification would be to reduce the antenna by some percentage and thereby push the dips to higher frequencies outside of the frequency band. Reducing the antenna size, however, would hinder the low frequency gain, so the reduction could not be too significant.

The size reduction was arbitrarily chosen to be 20%, which would shift the low frequency match from 350 to 420 MHz, and push the peak in gain at 850 MHz (Fig. 15) to above 1,000 MHz. The roll-off above 1,000 MHz could be tolerated, as long as the dip is not more than a few decibels isotropic. All dimensions were reduced by 20% with exception made to the CPW dimensions (spacing and width) and the substrate thickness. The CPW spacing was doubled and the width adjusted accordingly to allow for tolerances in manufacturing; see Fig. 22 for detailed dimensions. An additional 0.4 inch of board was further removed on either side of the feed, after scaling, to reduce, as much as possible, the impact of the ground width on the pattern bifurcation. Figure 23 shows the size comparison between the first and second revisions.

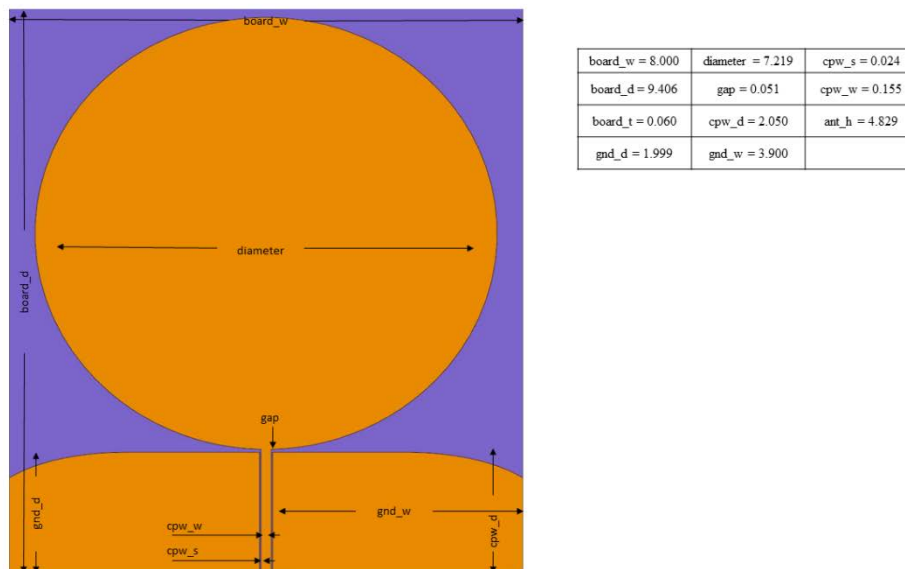


Fig. 22 Second revision dimensions (in inches) with a measurement accuracy within ± 0.005

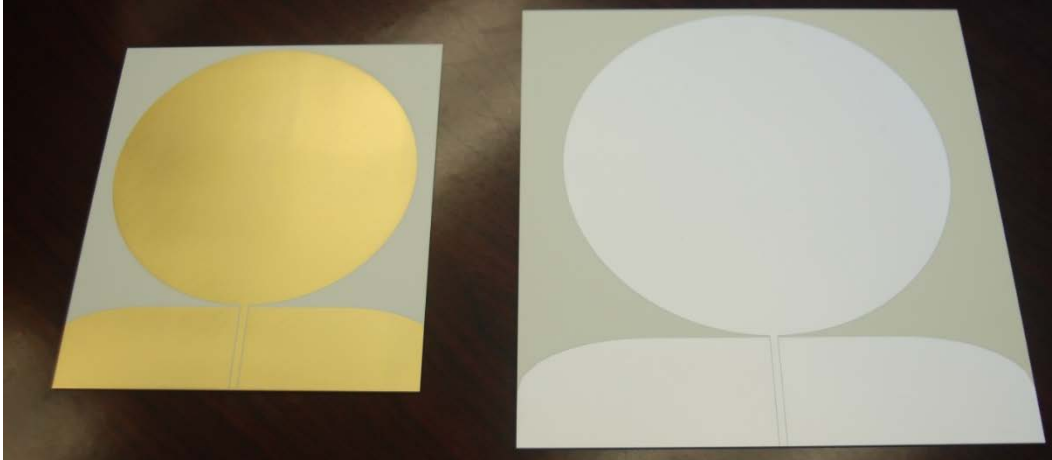


Fig. 23 Size comparison of the first (right) and second (left) UWB-CPM revisions

The second revision is well matched from 450 to 1,200 MHz as expected (Fig. 24), and the realized gain has its peak shifted to above 1,000 MHz, as expected (Fig. 25). The return loss for the second revision with the enclosure (Fig. 26) shows that the new antenna is no longer well matched with the current enclosure configuration. The enclosure wall closest to the antenna is the culprit for the poor match. While the matching is poor, the gain dips that were present in the first revision are no longer present for the second revision (Figs. 27 and 28). Reducing the antenna's size by 20% and removing some of the excess board on the sides of the antenna has led to an improvement in the realized gain. The gain variation is now 6 dB on boresight and 9 dB tilted versus 16 dB for both cases with the previous revision.

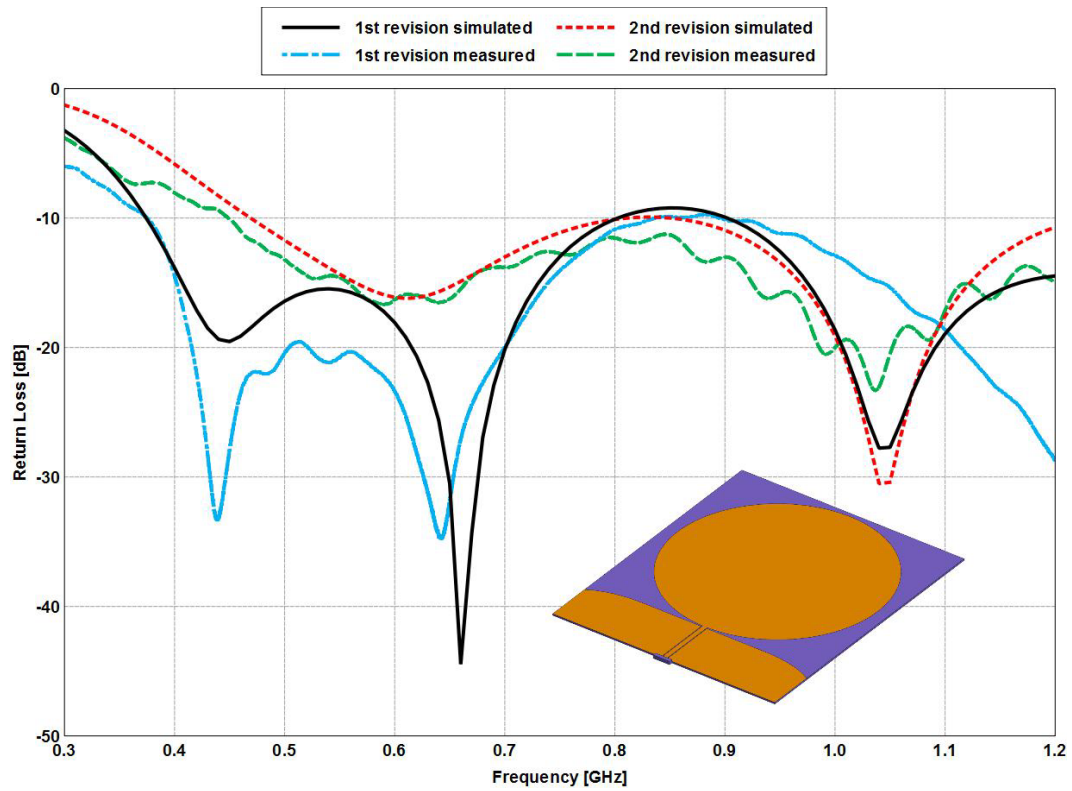


Fig. 24 Simulated and measured return loss for the first and second revision

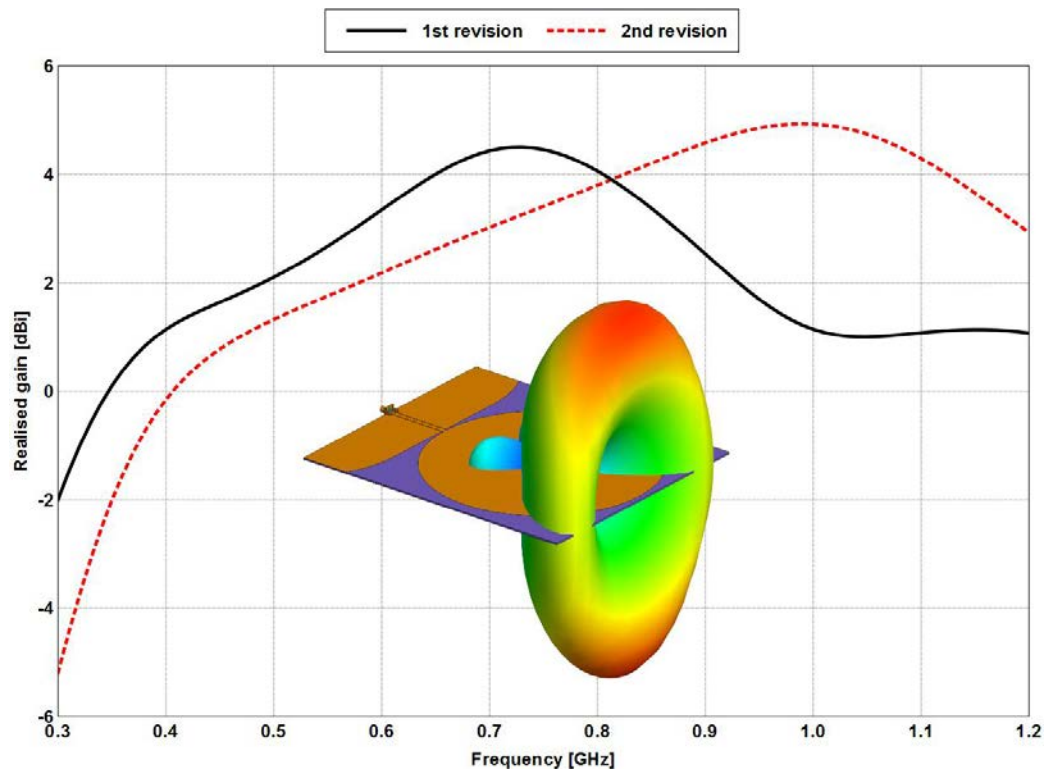


Fig. 25 Simulated realized gain for the first and second revision at $\theta = 30^\circ$ and $\phi = 90^\circ$

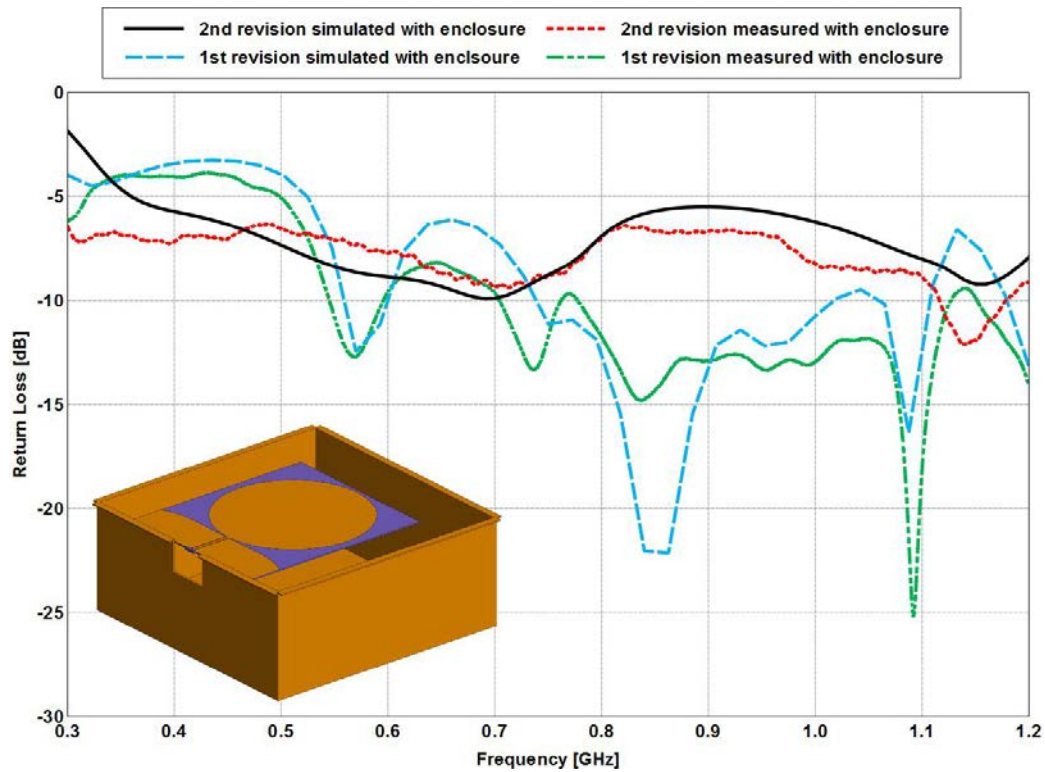


Fig. 26 Simulated and measured return loss for the first and second revisions with an enclosure

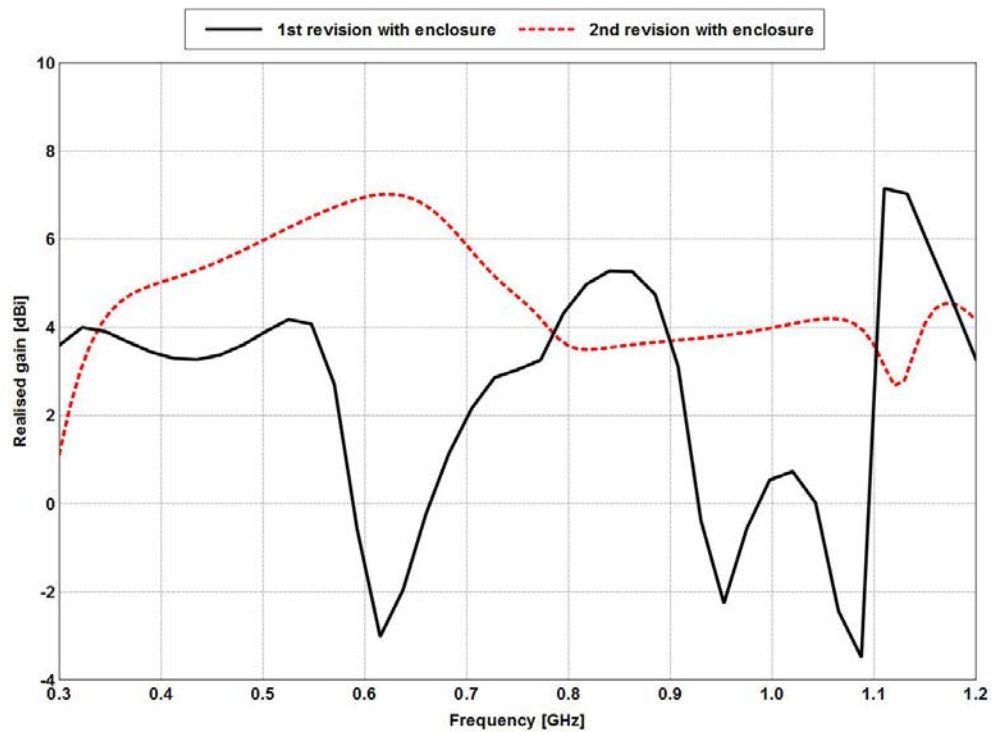


Fig. 27 Simulated realized gain for the first and second revision with an enclosure at $\theta = 0^\circ$ and $\phi = 90^\circ$

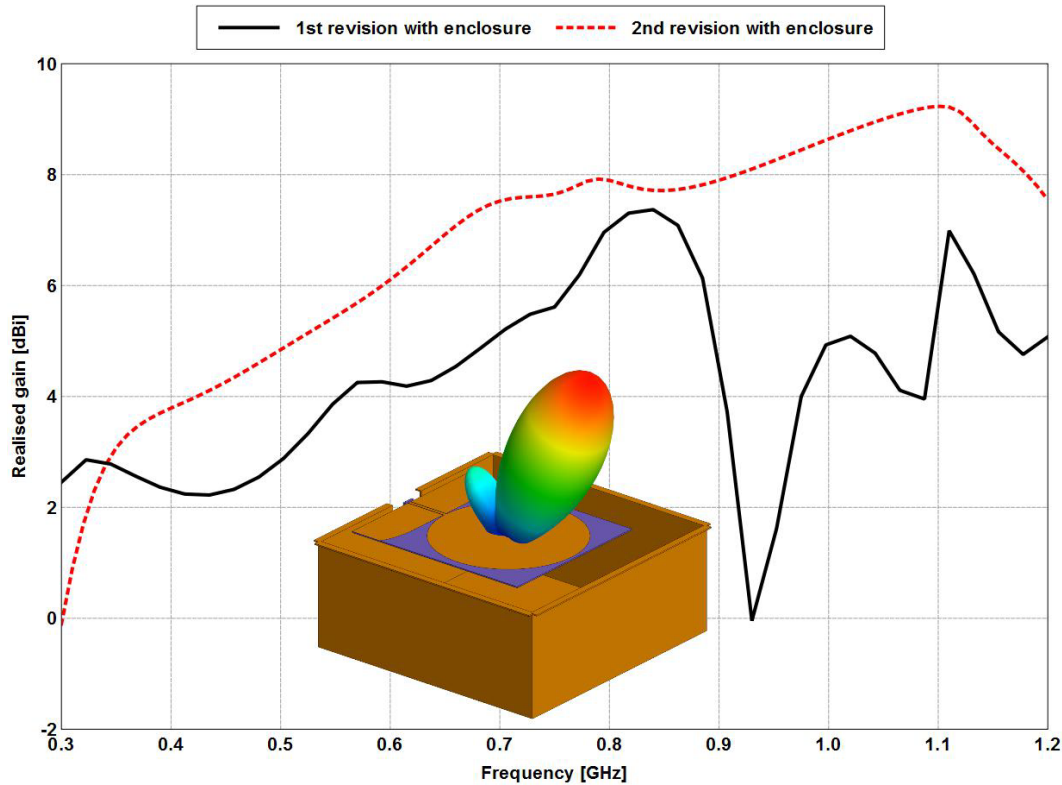


Fig. 28 Simulated realized gain for the first and second revision with an enclosure at $\theta = 30^\circ$ and $\phi = 90^\circ$

Even though the return loss is poor, the realized gain is high without any serious dips. The electric current distribution comparison between the first and second revisions at 950 MHz (Fig. 29) shows that the size reduction has significantly reduced the antenna and enclosure interaction. The amount of current on the top edge and sides of the enclosure is significantly smaller than for the first revision. This translates to a radiation pattern that is no longer bifurcated at that frequency. Figure 30 shows the linear radiation pattern at 950 MHz for the first and second revisions. Clearly, the radiation pattern is no longer bifurcated in the forward direction, and the feed facing lobe has also been unexpectedly reduced, as well, which translates into a larger forward gain.

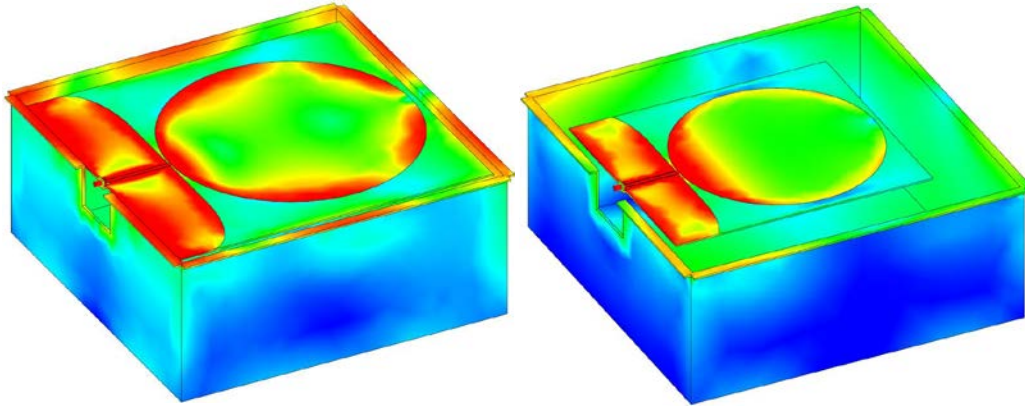


Fig. 29 First (left) and second revision (right) electric current distribution at 950 MHz

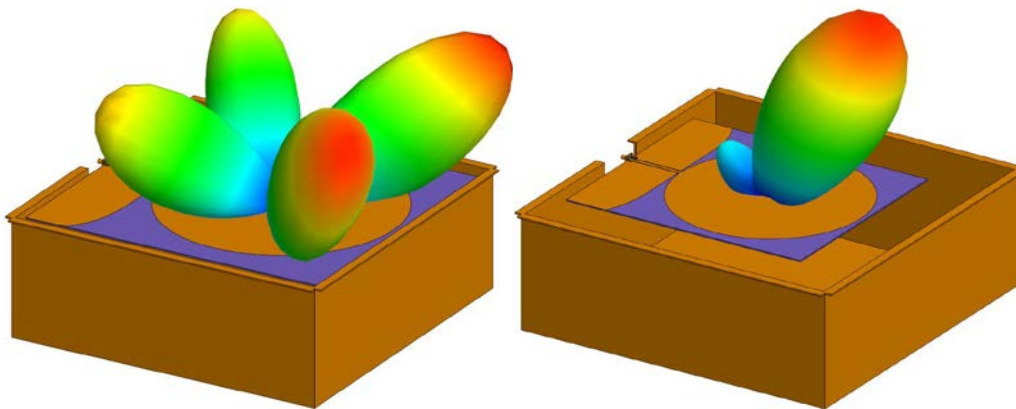


Fig. 30 First (left) and second revision (right) linear radiation patterns at 950 MHz

The metallic enclosure, just as with the first revision, serves to improve the isolation (S21 measurement) between the 2 antennas (Fig. 31). Just as with the first revision, the measurement was made under anechoic conditions with the antennas positioned 13.5 inches from each other measured center-to-center. The inclusion of the metallic enclosure improves the S21 by at least 6 dB at low frequencies and 10 dB at higher frequencies. There are some frequencies where the enclosure does not improve the S21, but, as stated previously, this is due to a resonant effect of the enclosures and the interaction between them. Including the radome did not have much of an impact on the S21, with the exception of below 350 MHz, where the polycarbonate appears to help to improve the isolation between the elements.

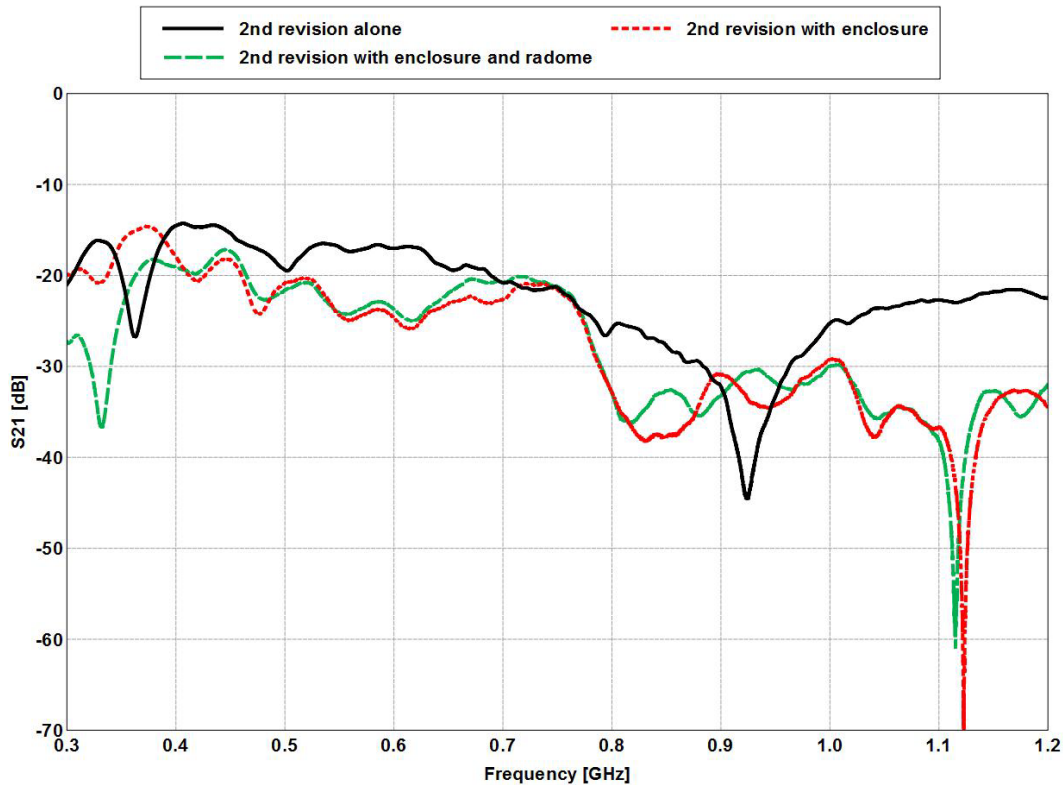


Fig. 31 Second revision UWB-CPM S21 measurement without an enclosure, with an enclosure, and with a radome

7. Second Revision UWB-CPM versus the Vivaldi

As shown in Section 3, the Vivaldi Aerial is an excellent candidate for broadband, directional applications when antenna size is not a concern. When antenna size is a concern, however, the Vivaldi can be undesirable as it can be at least one wavelength in length and one half-wavelength in width. The Vivaldi example in Section 3 (which is not the same as the current Vivaldi antenna) showed excellent performance for the 300 to 1,200 MHz frequency band, but was significantly larger than the UWB-CPM.

Figure 32 shows the return loss for the second revision UWB-CPM (first-generation UWB-CPM) and the example Vivaldi. Clearly, the example Vivaldi is superior to the UWB-CPM across the frequency band. Naturally, the good return loss translates into a good VSWR (Fig. 33), where the Vivaldi has a value of less than 2 across the frequency band (it is 2.1 just below 400 MHz), whereas the UWB-CPM is less than 3.5 from 350 to 1,200 MHz. The example Vivaldi also has larger gain than the UWB-CPM by about 2–3 dBi (Fig. 34). However, the example Vivaldi has a length that is 4 to 8 times larger (depending on if the UWB-CPM is titled) and a width that is 2 times larger than the CPM. If the VSWR can be

tolerated, the UWB-CPM would be the preferred antenna for a low profile application. There is good agreement between the measured and simulated results for the UWB-CPM since the unexpected dips and peaks in gain are not due to the antenna, but are caused by the anechoic environment in which measurements were taken. Gain calibration only calibrates out the response of the chamber to the calibration standard antenna pattern (in this case, a ridged horn), but does not calibrate out the response of the chamber to the antenna under test pattern.

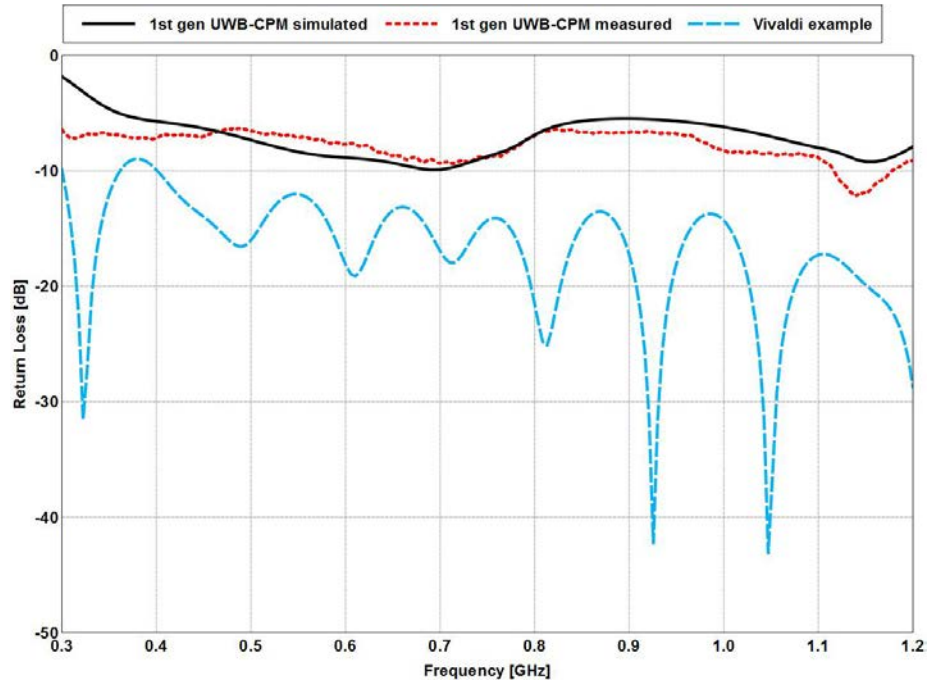


Fig. 32 Simulated and measured return loss for the first-generation UWB-CPM and the Vivaldi example

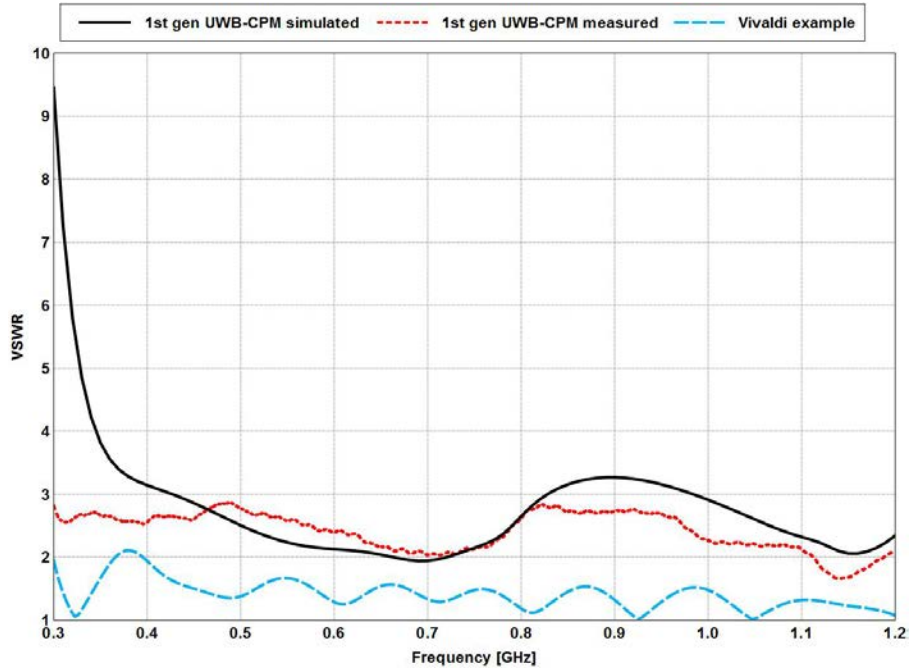


Fig. 33 Simulated and measured VSWR for the first-generation UWB-CPM and the Vivaldi example

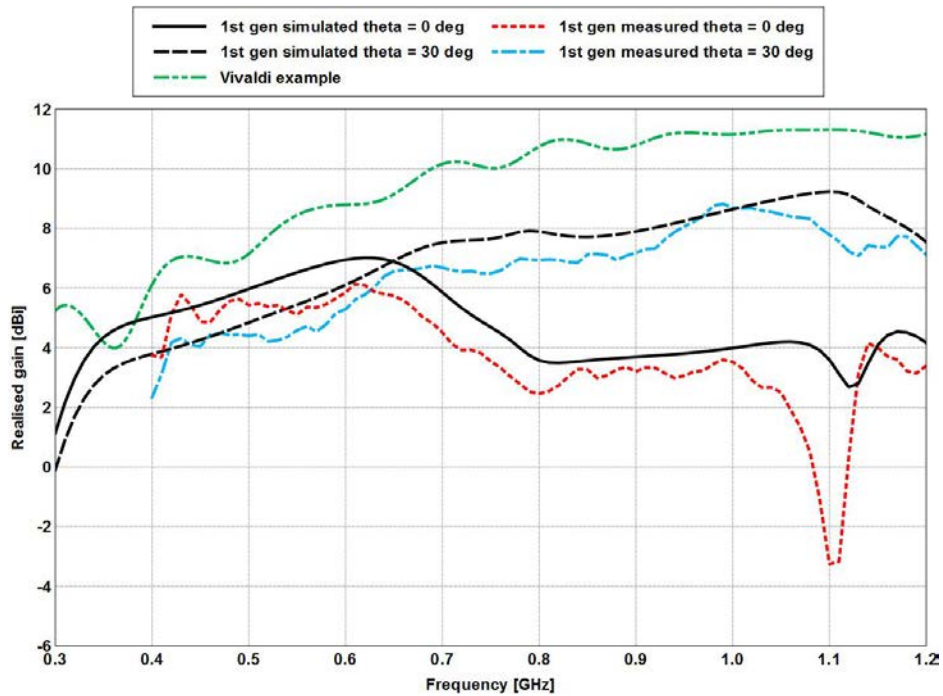


Fig. 34 Simulated and measured realized gain for the first-generation UWB-CPM and the Vivaldi example

The current Vivaldi antenna dimensions are smaller than the example Vivaldi. Because of the smaller length and width, the current Vivaldi performs better at

higher frequencies, but is outperformed by the UWB-CPM for the entirety of the 300 to 1,200 MHz frequency band. The current Vivaldi was lengthened to help improve the impedance match for 300 to 1,200 MHz, giving it an improved VSWR for most of the frequency band, but the UWB-CPM is superior in both VSWR and gain.¹ The UWB-CPM has much larger gain than the current antenna, both on boresight and at a E-plane tilt angle of 30°, and the vertical profile is smaller by about 40% when tilted and even more so when not. Figure 35 shows the simulated models for the final UWB-CPM next to the Vivaldi example to highlight the size difference between a 300 MHz Vivaldi and the UWB-CPM, and Fig. 36 shows the UWB-CPM and dual-pol configured Vivaldi example. Figure 36 highlights the end result advantage of the proposed antenna in this report, as later generations of the UWB-CPM will incorporate dual-pol features within the same package.

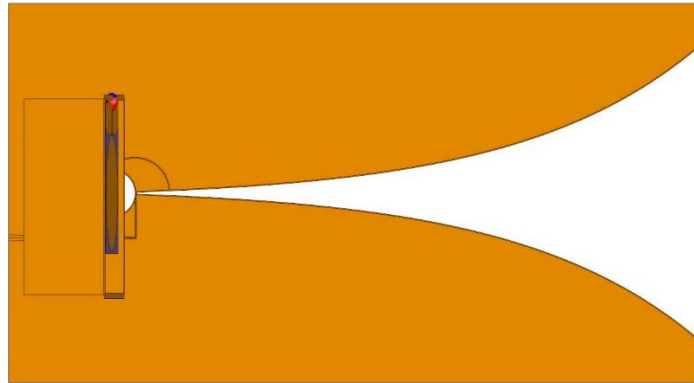


Fig. 35 First-generation UWB-CPM and Vivaldi example size comparison

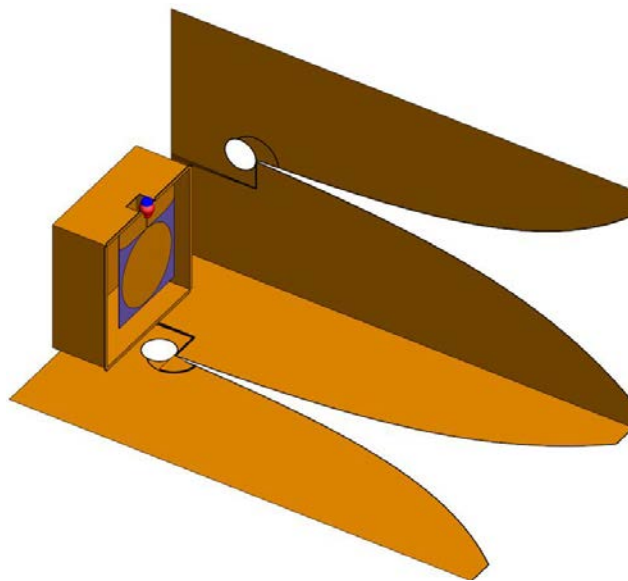


Fig. 36 First-generation UWB-CPM and example Vivaldi antenna in dual-pol configuration size comparison

8. Summary and Conclusions

The UWB-CPM presented in this report provides an alternative to an already-existing Vivaldi antenna.¹ Vivaldi antennas are ideal for directional, broadband applications, but are very large with a high aspect ratio. The current Vivaldi antenna operates best in a frequency band above 1,200 MHz due to the small dimensions producing low gain between 300 and 1,200 MHz and a poor VSWR as well. The vertical profile is also larger in comparison to the UWB-CPM. An example Vivaldi antenna was designed and simulated for the frequency band of 300 to 1,200 MHz to show that the antenna has the potential to perform very well for broadband, high gain systems, but the good performance is accompanied with a large size that make the Vivaldi unsuitable for low profile (compact) applications. The goal of the UWB-CPM is to offer a lower profile alternative with better performance than the current system.

Because of the multi-channel configuration of the existing platform, where each antenna is sampled individually but arranged in an array-like fashion, minimizing the mutual coupling had to be kept in mind when designing the UWB-CPM. The baseline UWB-CPM configuration consisted of a 12 inch x 12 inch quarter-wave reflector backing a basic UWB-CPM with a plastic enclosure. The baseline antenna performed well across the band, with the exception of poor gain at low frequencies due to the reflector being too small. Additional concerns were with the sturdiness of the plastic enclosure, weight, and mutual coupling.

The goal of the first revision of the UWB-CPM was to address the issues that became apparent in designing the baseline. Substituting a welded aluminum enclosure for the intended plastic enclosure solved the problem of the low gain at low frequencies, but introduced additional issues with the gain. Naturally, the metallic enclosure harmed the return loss so that only 81% of the impedance bandwidth was retained, but the metallic walls improved the S21 such that the isolation was 20 dB or better across the frequency band versus 13 dB or better without the enclosure. Maintaining a rigid support for the end launch connector was critical to the performance of the fabricated antenna. The outer conductor had to be kept isolated from the walls of the enclosure while maintaining a rigid structure, so a cutout with a U-shaped brass piece bolted to a sheet of G10 served the purpose.

The roll-off in gain at 600 MHz due to the pattern tilt became more exaggerated due to the enclosure, but could be rectified by scanning off boresight by 30° away from the feed (E-plane). The interaction between the antenna and enclosure resulted in severe pattern bifurcation at 950 and 1,050 MHz. Any UWB-CPM has some pattern bifurcation, but the current on the outer edges of the enclosure exaggerated the bifurcation such that the gain would dip by as much as 7 dBi or more. Even

though the metallic enclosure did improve the isolation, low frequency gain, and ruggedness of the antenna platform, the dips in gain could not be tolerated and had to be corrected.

The goal of the second revision of the UWB-CPM was to address the gain dips caused by the interaction between the antenna and enclosure. Attempts to modify the enclosure in such a way as to lengthen or shorten the current paths failed. Notching the enclosure walls would have an obvious effect on the radiation pattern and impedance, but no combination of notches, sizes, or positions attempted would improve the bifurcated pattern. Simulations with absorber-treated enclosure edges were not successful either. The only way to address the bifurcation was to modify the antenna to push the bifurcation to higher frequencies.

A reduction factor of 20% was applied to the first revision, with an additional removal of 0.4 inch of board on either side of the antenna to further reduce the width of the ground plane as much as possible. The reduction of the antenna led to a significant improvement in gain across the frequency band and solved the bifurcation problem in the frequency band of interest. However, the second revision did lose a good impedance match across the entire bandwidth with a return loss -6 dB or better from 400 to 1,200 MHz. The gain improvement of about 2 dBi across the frequency band (with an increase from 0 dBi at 300 MHz to 9 dBi at 1,100 MHz followed by a dip of 1.5 dBi) can justify the poor match. Just as with the first revision, the enclosure for the second revision improved the isolation by about 6 to 10 dB at most frequencies.

The second revision meets nearly every goal with the exception of a good impedance match across the frequency band, but the high gain can make the tradeoff potentially worth it. Compared to the example 300 MHz Vivaldi, the UWB-CPM does not perform as well, but is much smaller in size. The actual Vivaldi antenna is smaller than the example Vivaldi, producing gain that is many decibels less than the final UWB-CPM with a poorer VSWR for the entirety of the frequency band. Also, the vertical profile of the UWB-CPM is at least 40% smaller (when tilted) than the current Vivaldi.

Future revisions will focus on improving the design and include the additional feature of dual polarization (switched vertical and horizontal or dual 45° slant). Integrating these later generations within a metallic enclosure will pose a significant challenge and may require some tradeoffs to be accepted. A prototype of the dual slant method has already been constructed for testing and model validation. The performance improvement of the cavity-backed UWB-CPM and dual-pol UWB-CPM will be the subject of a follow-on report.

9. References

1. Smith GD, Harris RW, Ressler MA, Stanton B. Wideband Vivaldi notch antenna design. Adelphi (MD): Army Research Laboratory (US); 2008 March. Report No.: ARL-TR-4409.
2. Zaghloul AI, Lee YM, Mitchell GA, Anthony TK. Enhanced ultra-wideband (UWB) circular monopole antenna with electromagnetic band gap (EBG) surface and director. Adelphi (MD): Army Research Lab (US); 2014 August. Report No.: ARL-TR-7041.
3. Volakis JL. Antenna Engineering Handbook. 4th ed. New York (NY): McGraw-Hill; 2007. p. 24.16–24.18 and 37.11–37.20.
4. FEKO. Stellenbosch (South Africa): Altair Engineering Inc.; 2015 [accessed 2016]. www.feko.info.
5. Stutzman WL, Thiele GA. Antenna Theory and Design. 3rd ed. Edison (NJ): John Wiley and Sons; 2013. p. 78–81 and 264–265.
6. Balanis CA. Antenna Theory. 3rd ed. Edison (NJ): John Wiley and Sons; 2005. p. 499.
7. Ray KP. Design aspects of printed monopole antennas for ultra-wide band applications. Intl J Antennas Prop. 2008. Hindawi Publishing Corporation.
8. Sayidmarie KH, Fadhel YA. Design aspects of UWB printed elliptical monopole antenna with impedance matching 2012. Proceedings of 2012 Loughborough Antennas & Propagation Conference; 12–13 Nov. 2012; Loughborough (UK).
9. Weng YF, Cheung SW, Yuk TI. Effects of ground-plane size on planar UWB monopole antenna. Paper presented at: TENCON; 2010.
10. Lu Y, Huang Y, Chattha HT, Cao P. Reducing ground-plane effects on UWB monopole antennas. IEEE Ant Wireless Prop Letters. 2011;10.
11. Gibson PJ. The Vivaldi Aerial. Paper presented at: 9th Eur. Microw. Conference; 1979; Brighton (UK). p. 101–105.
12. Yngvesson KS, Schaubert DH, Korzejiowski TL, Kollberg EL, Thungren T, Johansson JF. Endfire tapered slot antennas on dielectric substrates. IEEE Trans On Ant Prop. Dec 1985;AP-33(12).
12. Shin J, Schaubert DH. A parameter study of stripline-fed Vivaldi notch-antenna arrays. IEEE Trans. On Ant. Prop. May 1999;47(5).

14. Antenna Magus. Antenna Magus; 2105 [accessed 2015].
www.antennamagus.com.

INTENTIONALLY LEFT BLANK.

Appendix. Detailed Drawings for Each Piece of the Enclosure

Ø0.113 THRU
100° CSK Ø0.225
COUNTERBORE ON INTERNAL SURFACE
16 PLCS

DETAIL "A"

2.56UNC2B 7 PLCS

NOTES

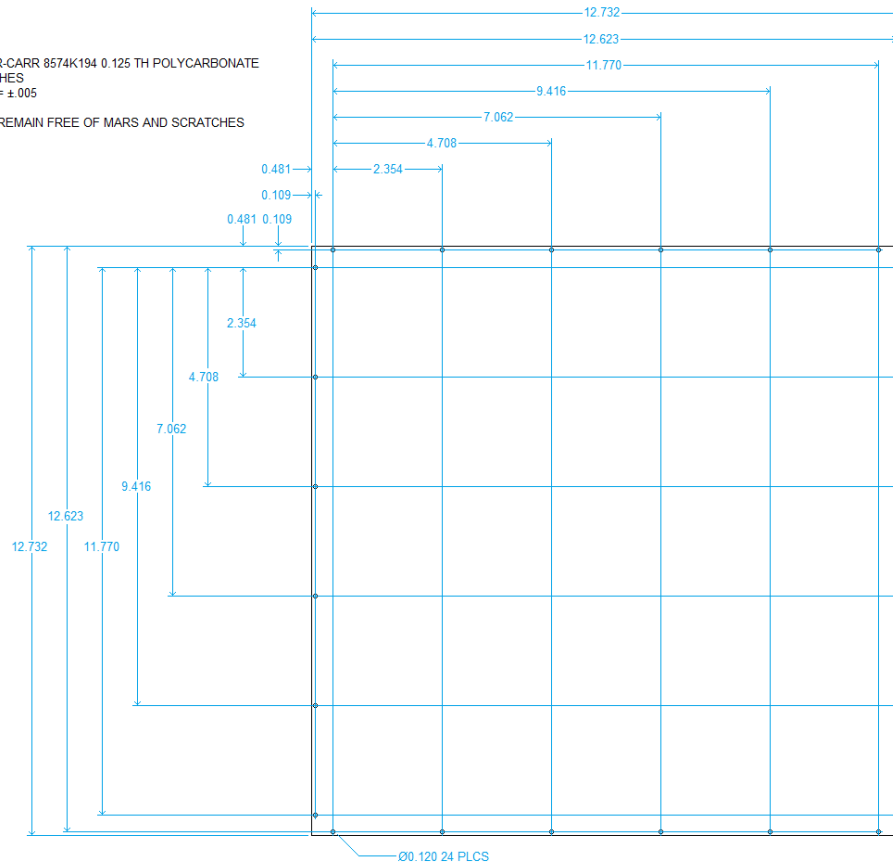
1. FABRICATE FROM FURNISHED ITEM
2. DIMENSIONS IN INCHES
3. TOLERANCE: .XXX = ±0.005
4. BREAK ALL EDGES
5. 1 PER UNIT

ENCLOSURE
REV 1 20151111

Approved for public release; distribution unlimited.

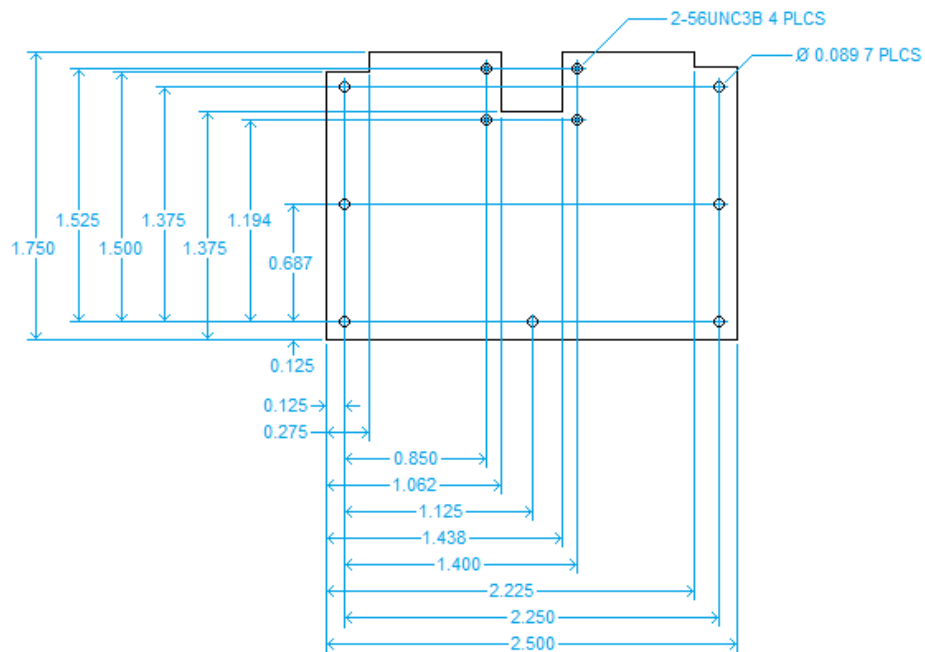
NOTES

1. MATL = MCMASTER-CARR 8574K194 0.125 TH POLYCARBONATE
2. DIMENSIONS IN INCHES
3. TOLERANCE: .XXX = ± 0.005
4. BREAK ALL EDGES
5. SURFACES SHALL REMAIN FREE OF MARS AND SCRATCHES
6. 1 PER UNIT



COVER
20151119

Fig. A-2 Enclosure cover

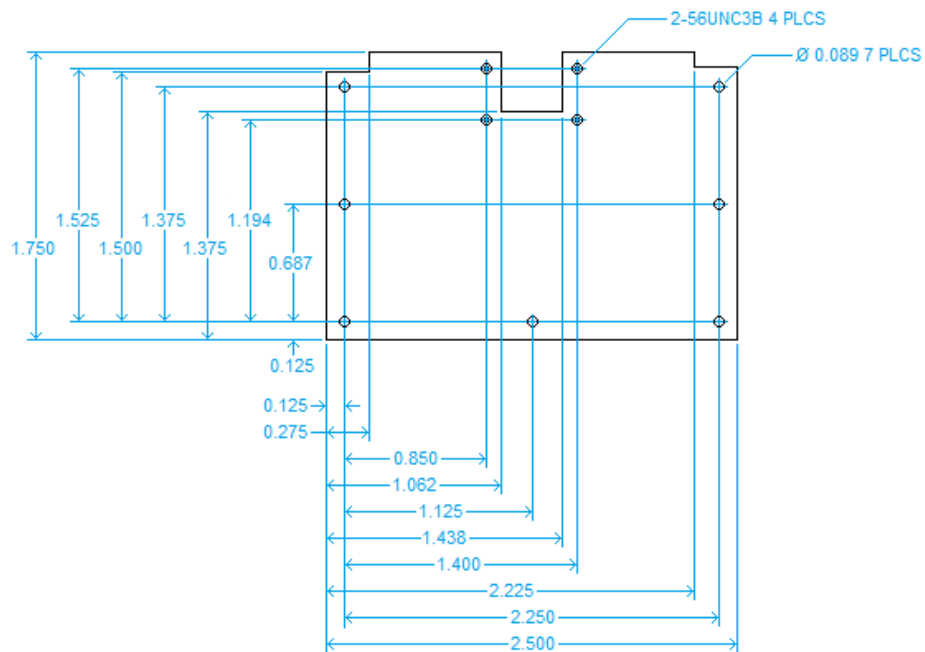


NOTES

1. MATL = 0.062 TH GLASS EPOXY
2. DIMENSIONS IN INCHES
3. TOLERANCE: .XXX = ± 0.005
4. BREAK ALL EDGES
5. 1 PER UNIT

CONNECTOR ISOLATION PLATE
REV. 2 20151223

Fig. A-3 Enclosure connector isolation plate, part 1

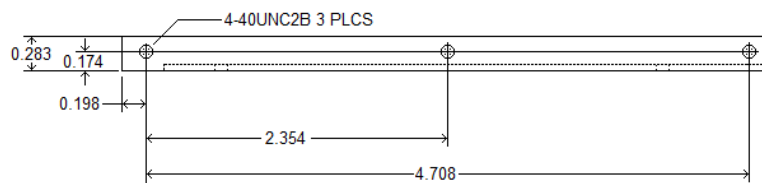
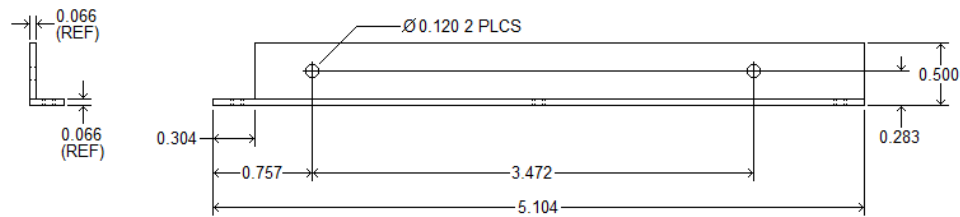


NOTES

1. MATL = 0.062 TH GLASS EPOXY
2. DIMENSIONS IN INCHES
3. TOLERANCE: .XXX = ± 0.005
4. BREAK ALL EDGES
5. 1 PER UNIT

CONNECTOR ISOLATION PLATE
REV. 2 20151223

Fig. A-4 Enclosure connector isolation plate, part 2

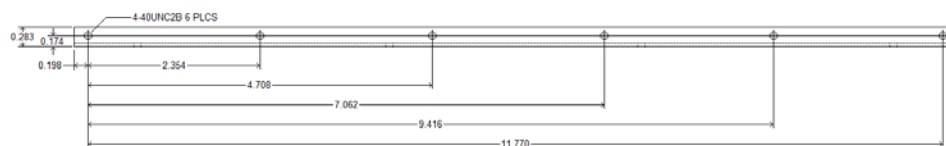
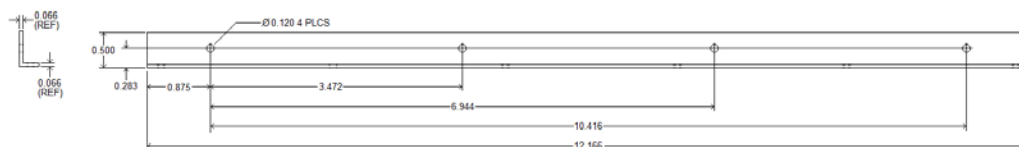


NOTES

1. FABRICATE FROM McMASTER-CARR 88805K68
2. DIMENSIONS IN INCHES
3. TOLERANCE: .XXX = ± 0.005
4. BREAK ALL EDGES
5. 1 PER UNIT

LEFT SHORT SUPPORT BRACKET, COVER, ANTENNA
20151117

Fig. A-5 Enclosure short support cover bracket, left



NOTES

1. FABRICATE FROM McMASTER CARR 88805K68
2. DIMENSIONS IN INCHES
3. TOLERANCE: .XXX = ± 0.005
4. BREAK ALL EDGES
5. 3 PER UNIT

LONG SUPPORT BRACKET, COVER, ANTENNA
20151116

Fig. A-6 Enclosure long support cover bracket

List of Symbols, Abbreviations, and Acronyms

3-D	3-dimensional
CEM	computational electromagnetic modeling
CPM	circular planar monopole
CPW	co-planar waveguide
dual-pol	dual-polarized
E	electric
EBG	electromagnetic bandgap
FBR	front-to-back ratio
GPR	ground penetrating radar
H	magnetic
MoM	Method of Moments
TEM	transverse electromagnetic
UWB	ultra-wideband
VSWR	voltage standing wave ratio

1 DEFENSE TECH INFO CTR
(PDF) DTIC OCA

2 US ARMY RSRCH LAB
(PDF) IMAL HRA MAIL & RECORDS MGMT
RDRL CIO LL TECHL LIB

1 GOVT PRNTG OFC
(PDF) A MALHOTRA

6 US ARMY RSRCH LAB
(PDF) RDRL SER M
S MCCORMICK
A ZAGHLOUL
A HARRISON
S WEISS
E ADLER
W COBURN